Using strontium in otoliths to determine the natal origin and habitat use of sockeye salmon in the Nushagak River

Final Report to Bristol Bay Regional Seafood Development Association

October 1, 2017

Sean R. Brennan and Daniel E. Schindler
University of Washington, School of Aquatic and Fishery Sciences

Diego P. Fernandez
University of Utah, Department of Geology and Geophysics

Executive Summary

The Nushagak River supports commercially, socially, and ecologically important runs of sockeye salmon that spawn and rear throughout this vast watershed. Adult fish are captured by commercial and subsistence fisheries in the lower river and estuary on their way to spawning grounds throughout the river basin. Because of the complexity and remoteness of this river system, the contributions of fish from different habitats to the fisheries remain poorly understood. Further, whether sockeye salmon production patterns across the watershed are relatively constant through time is also not understood. In this project we refined a spatial model characterizing strontium isotope ratios throughout the Nushagak River to provide a baseline to be used to assign fish caught in the lower river and estuary to their natal habitats. Because ear stones (otoliths) in salmon accumulate sequentially as a fish grows (similar to the rings of a tree) and reliably archive the strontium isotopes found in the water fish are living in at any point in time, otoliths from adult salmon can be analyzed to determine the birth location of fish caught in fisheries.

Strontium isotopes from otoliths of adult sockeye salmon, caught as they migrated past Portage Creek on the lower Nushagak River in 2014 and 2015 were used to assign individual fish to their natal geographic origins throughout the river basin. Sample sizes were 262 and 296 sockeye salmon in 2014 and 2015, respectively. In 2014, most sockeye salmon were inferred to be returning to spawn in Nuyakuk Lake, the King Salmon River, and the upper and middle stems of the Nushagak River; contributions from the lower Nushagak and the Mulchatna Rivers were relatively small. In 2015, sockeye salmon were inferred to be returning to spawn throughout a much larger fraction of the Nushagak basin than in 2014. In particular, contributions from the Mulchatna River and the lower Nushagak River were substantially more important in 2015 compared to 2014.

These results emphasize that sockeye salmon are produced by most of the lake and river habitat found in the Nushagak River basin. Importantly, however, not all habitat supports substantial production in any given year. Rather, Nushagak River sockeye salmon are produced by a spatial mosaic of habitats whose profitability shifts from year to year, presumably in response to interactions between local habitat conditions and overriding environmental forcing (e.g., temperature and precipitation patterns). These results emphasize the importance of habitat complexity for stabilizing production of sockeye salmon through time from this, and other, river ecosystems. Environmental impact assessments of potential development activities must take into account the fact that habitat conditions are continuously varying and that the importance of any component of habitat can be disproportionately important for sustaining fisheries in some years, even if their average contribution are small over the long-term. Thus, maintenance of the habitat complexity across the river basin should be made a conservation priority for the Nushagak River, if sustaining reliable commercial and subsistence fisheries are a long-term goal for management.

Project Description and Objectives:

The Nushagak River is a vast watershed that supports commercially and socially important fisheries for sockeye salmon. However, it remains unclear which regions of the Nushagak watershed produce the majority of sockeye salmon, and whether the contributions of production from different tributaries varies through time. Recent research (Brennan et al. 2015b) shows that naturally occurring geochemical tracers in Nushagak River waters enable determination of the natal origins of Chinook and sockeye salmon. The most powerful tracer is the ratio of two isotopes of the trace element strontium (Sr), which is incorporated from river waters into juvenile salmon otoliths (ear-stones), which provide a chemical history of each fish's entire life. A baseline dataset quantifying the strontium ratios of potential habitats for sockeye salmon was refined and used to identify which regions of the Nushagak produce the most fish.

The objectives of this project were to **1)** fill in data gaps describing the water chemistry in the Tikchik Lakes region of the Nushagak basin, **2)** finalize a geospatial model of Sr isotope ratios across the Nushagak River able to determine the natal origins of this river's sockeye salmon populations, and **3)** apportion the sockeye salmon returning in 2014 and 2015 to the Nushagak River using this geospatial model in order to elucidate the production patterns of salmon across the basin and among years.

Methods:

During the summer of 2014 we collected samples of river and lake waters from throughout the Tikchik Lakes region to supplement the isotope baseline we had previously developed for other parts of the watershed (Brennan et al. 2015a). The strontium concentrations [Sr] (mg/L) and the strontium isotope ratios ($^{87}Sr/^{86}Sr$) of these waters were measured at the University of Utah, Department of Geology and Geophysics, Inductively Couple Plasma Mass Spectrometry (ICPMS) laboratory using both single-collector (SC) and multi-collector (MC) instruments, respectively. Using these data, plus the existing dataset across the Nushagak River basin (Brennan *et al.* 2015a), we generated a dendritic strontium isoscape, which predicted the $^{87}Sr/^{86}Sr$ ratios of river waters throughout the river network (Brennan *et al.* 2016). This model used a new class of geostatistical models that were built specifically for river networks, Spatial Stream Network Models (Peterson & Ver Hoef 2010; Ver Hoef & Peterson 2010).

To demonstrate that dendritic isoscapes can accurately and precisely determine the natal origins of salmon produced from throughout the Nushagak River, we blindly determined the natal origins of known-origin juvenile Chinook salmon with >95% accuracy (correct geographic assignments of fish) and <4% precision (in terms of the proportion of habitat representing the natal origin relative to total) (Brennan & Schindler 2017). This model was then applied to a mixed-stock fishery sample of adult Chinook salmon captured in the Nushagak Fishing District during the 2011 return of Chinook salmon to the Nushagak River. By determining the natal origins of these adult Chinook salmon harvested in Nushagak Bay on the basis of strontium isotopes in otoliths, we were able to map the heterogeneous production patterns of the 2011 return (Brennan & Schindler 2017).

Once the above modeling framework was in place (Brennan *et al.* 2016; Brennan & Schindler 2017), we applied the same methodology to sockeye salmon collected by the Alaska Department of Fish & Game at the Portage Creek sonar site on the lower Nushagak River in years 2014 and 2015. Migrating adult sockeye salmon were collected from the sonar site to ensure that the sample was composed of those fish bound for habitats within the Nushagak River basin. A collection from the Nushagak Fishing District would have included fish bound for the Wood and Igushik rivers. Individuals were collected over the course of the run for each year (Figure 1). These collections were then grouped into time strata, which were used to weight the geographic assignments of fish sampled within each strata so as to account for any difference in timing among geographically disparate, and therefore isotopically distinct, regions.

Specifically, all fish within a time strata were assigned to their most likely natal origins and then multiplied by the number of fish that passed the sonar during that same time strata. Weighting by the escapement instead of the total run (i.e., escapement+harvest) potentially introduced a temporal bias in our estimates if there was a significant timing difference between when fish entered the Nushagak Fishing District versus when they passed the sonar site. However, estimates for harvests solely on Nushagak River sockeye salmon are currently not available (Tyler Dann, ADFG, personal communication).

The sockeye salmon assignment model uses the dendritic isoscape model (Figure 2) to evaluate the most likely geographic locations given the isotope signature measured in an otolith and those signatures predicted throughout the river system. A useful feature of using a Bayesian assignment framework is that habitat suitability indicators determined by GIS can be used as Bayesian 'priors' to complement the geographic assignments using habitat data beyond the strontium isotopes (Brennan & Schindler 2017). Because different species of salmon exhibit preferences for geomorphic features of rivers systems, and because some portions of a river system may be upstream of barriers to migration – such priors can be highly informative. Here, we used a uniform habitat prior that essentially required those lakes or reaches of rivers situated upstream of a barrier to salmon migration to have probability of zero and all other reaches downstream of such barriers to migration to have equal *a priori* probabilities (i.e., probability of 1). One known barrier to migration in the Nushagak River is the falls in the Allen River, which connects Chikuminuk Lake to Lake Chauekuktuli. As such, all habitats above this falls were assumed to produce zero sockeye salmon. Because 0 freshwater-age (e.g. 0.3 or 0.4) sockeye salmon can make up a substantial portion of the sockeye salmon produced out of the Nushagak River, we did not use a prior that would distinguish lake versus river habitats, assuming that 0 freshwater age sockeye salmon usually exhibit a sea-type life history (typically characterized by riverine habitat use).

Otoliths from adult sockeye salmon captured at Portage Creek sonar site were mounted on petrographic slides and ground down in the sagittal plane to the otolith core in order to reveal the entire growth history of each individual. After polishing, these sections were sonicated in ultrapure MilliQ water to clean the exposed otolith surface. Using laser ablation (LA) MC-ICPMS, the $^{87}Sr/^{86}Sr$ ratios were measured along the growth axis of each otolith using a 53um diameter beam and scanning at 2um/second. The laser energy was 3.23J/cm^2 while firing and was shot at 10Hz. The resulting data for each individual was an estimate of the $^{87}Sr/^{86}Sr$ ratios from the otolith core, through the entire freshwater residence period, and approximately 200um into the marine residence period. The natal region of the otolith was determined by correlating the $^{87}Sr/^{86}Sr$ ratios and ^{88}Sr (V) intensities (a proxy for the amount of Sr) with the otolith growth structure in order to identify the point at which the otolith was first in equilibrium with the ambient water of its natal habitat. This equilibrium usually occurred between 250-300 um from the core's primordia, a feature also visually discernable in the otolith growth structure. The egg from which a salmon hatches influences the core of its otolith, as such it is important to avoid this material when determining the natal region. The core material is inherited from an individual's mother and is ultimately from the ocean. Once identified, the $^{87}Sr/^{86}Sr$ ratios within the natal region were then used to determine a fish's natal origin using the above Bayesian assignment framework, which determines the most likely geographic locations within the river basin based on isotope information (i.e. the isotopes measured in the otolith and the isotopes predicted throughout the river network).

Results and Discussion:

The Nushagak River's Dendritic Strontium Isoscape

The additional measurements we made throughout the Tikchik Lakes region greatly improved the strontium isotope baseline of the Nushagak River filling in key data gaps, especially those related to sockeye salmon habitat. These measurements increased the total range of $^{87}Sr/^{86}Sr$ ratios by approximately 50%, lending even more power to this methodology to precisely and accurately determine the natal origins of salmon in the Nushagak. The geospatial model that analyzed these data and predicts Sr isotopes throughout the Nushagak River is outlined in detail in Brennan *et al.* (2016) and is also depicted in Figure 2. This dendritic isoscape forms the foundation of the isotope-based assignment model we developed during and used throughout this project and represents marked improvements in prediction accuracy (RMSPE = 0.0005) (Brennan *et al.* 2016) compared to other methods for building isoscapes of rivers (RMSPE = 0.0013) (Bataille & Bowen 2012; Bataille *et al.* 2014).

The Production Patterns of Nushagak River Sockeye Salmon in 2014 and 2015

1) Basin wide and inter-annual production patterns:
Production patterns of sockeye salmon were spatially distributed throughout the Nushagak basin in both 2014 and 2015, though the spatial distribution was different in these two years (Figure 3 and 4). For fish returning in 2014, the production of sockeye salmon was highly concentrated in the Tikchik Lakes region, specifically Nuyakuk Lake (Figure 3). In 2015, however, the production was more evenly distributed throughout the basin, where habitats within the eastern parts of the basin (e.g., the Alaskan-Aleutian Range [AAR] tributaries and lakes, such as the Mulchatna, Chilikadrotna, and Koktuli) contributed substantially to the 2015 return. In 2015 these habitats were nearly twice as productive than they were in 2014 (Figure 4).

2) Production patterns among different freshwater age classes:
The Nushagak River is unique among the major rivers draining into Bristol Bay because it is composed of both large lakes and extensive riverine habitats. This diversity in habitat has led to all three of the general freshwater life history strategies, or eco-types, of sockeye salmon being expressed in the Nushagak River: 'lake-type' (sockeye that spend 1 or more years rearing in a lake before outmigration), 'river-type' (sockeye that spend 1 year rearing in riverine habitats), and 'sea-type' (sockeye that migrate to the sea as sub-yearlings). Here, we assume that adults with a freshwater age of 0 were of the 'sea-type' life history, as these individuals migrated to sea as sub-yearlings; and those individuals with freshwater ages of 1 or 2 years were either 'lake' or 'river-type' sockeye, spending at least one full year in either a lake or riverine habitat. Sometimes river- and sea-type are grouped together given that both of these eco-types do not use lake habitats (Wood 2010), but we make the distinction here due to the substantial numbers of 0 freshwater age sockeye originating from the Nushagak basin.

In both years of returns, there were distinct differences in the production patterns of 0 freshwater age sockeye salmon (sea-type) versus those that spent at least one full year in freshwater before migrating to the ocean (lake or river type (Figure 5). The freshwater age 0 fish show much higher production out of riverine habitats, namely those of the Mulchatna basin. This is especially apparent in 2015, where the highest producing reaches of 0 freshwater age sockeye were from the Mulchatna River. Much of the difference in production between 2014 and 2015 is likely due to the strong return of 0 freshwater age fish, which originated largely from the Mulchatna River basin.

3) Patterns at the sub-basin geographic scale within the Nushagak:
Evaluating production at the scale of the major sub-basins within the Nushagak indicates that the

estimates herein scale positively with the proportion of habitat represented within a sub-basin (Figure 6 and Table 1). However, the isotope-based production estimates for sub-basins differ substantially from production estimates assuming that production of sockeye salmon is directly proportional to the amount of habitat available (Table 1). For example, the Nuyakuk Lake basin (excluding the Nuyakuk River) represents approximately 23% of the habitat available to sockeye salmon, but in both 2014 and 2015 its production was 49% and 35% of the basin wide total, respectively. This corresponds to a nearly 100% and 50% increase, respectively, in production compared to the amount of habitat available. Most of this difference is likely due to the relatively productive lake-associated life history of sockeye salmon. However, the substantial reduction in production from the Nuyakuk Lake basin in 2015 relative to 2014 levels was largely driven by a strong return of 0.3 fish (Figure 7), which originated primarily from isotopic regions not associated with large lakes and instead had isotopic signatures more aligned to the Mulchatna River and AAR tributaries. Habitats within these regions are largely composed of rivers and streams with some small spring-fed ponds (e.g. Swan River within the Koktuli River) and smaller lakes (e.g., Turquoise Lake). An example of a large lake system that showed relatively weak production, relative to its size, was Lake Chauekuktuli (i.e., production values 64% and 92% lower than an expectation based on basin size [its proportion of the total amount of habitat]). Lake Chauekuktuli and its northern tributaries are isotopically unique in the Nushagak (Figure 1) yielding a high degree of power and precision in determining its sockeye populations. Nonetheless, in both 2014 and 2015 there were relatively few sockeye salmon returning to Lake Chauekuktuli.

Conclusions:

The results of this project demonstrate how production of sockeye salmon throughout the Nushagak River basin is heterogeneous at multiple spatial and temporal scales. Production patterns within and among the years evaluated here illustrate the interplay between habitat and life history diversity, and how these components of salmon biology influence the overall production of sockeye salmon at regional scales (Schindler *et al.* 2010; Schindler, Armstrong & Reed 2015). Life history eco-types of sockeye salmon are locally adapted to different habitats (e.g., lakes versus rivers). Because the Nushagak basin is composed of both large lakes and vast rivers and streams the risk of a low return of sockeye salmon for any given year is spread across not just the differing life history strategies expressed throughout the basin, but also across its diverse habitats at multiple geographic scales. These findings emphasize how conserving both habitat and life history diversity within the Nushagak River basin is probably necessary to ensure reliable returns of salmon from this watershed. In the Nushagak, although the Tikchik Lakes region produced many of the fish in both 2014 and 2015, the riverine habitats throughout places such as the Mulchatna River represent important producers of a unique life history strategy that in certain years (e.g. 2015) can be particularly productive. Because the biodiversity of salmon is structured hierarchically in both space and time, salmon productivity is buffered against environmental changes, which can play out at multiple scales. By using strontium isotopes in otoliths of sockeye salmon we were able to unravel how these features of salmon biology contribute to the inter-annual variation in sockeye salmon to the Nushagak basin.

Acknowledgements:

This research was supported primarily by a grant from the Bristol Bay, Regional Seafood Development Association. We thank Greg Buck and field team from ADFG for collecting otoliths from sockeye salmon at the Portage Creek sonar site on the Nushagak River. Jenna Keeton and Jeff Baldock assisted with the lab work involved in this research.

Figure 1: Run timing in years 2014 and 2015 of i) harvest in the Nushagak Fishing District (black line), ii) escapement into the Nushagak River counted at the Portage Creek sonar site (red line), iii) samples used for the herein analysis (blue circles; size of circle scales with number of samples in strata) to determine natal origins and production patterns of sockeye salmon. Vertical black lines denote the time strata used to weight the geographic assignments by the number of sockeye salmon that passed the sonar for a given strata.

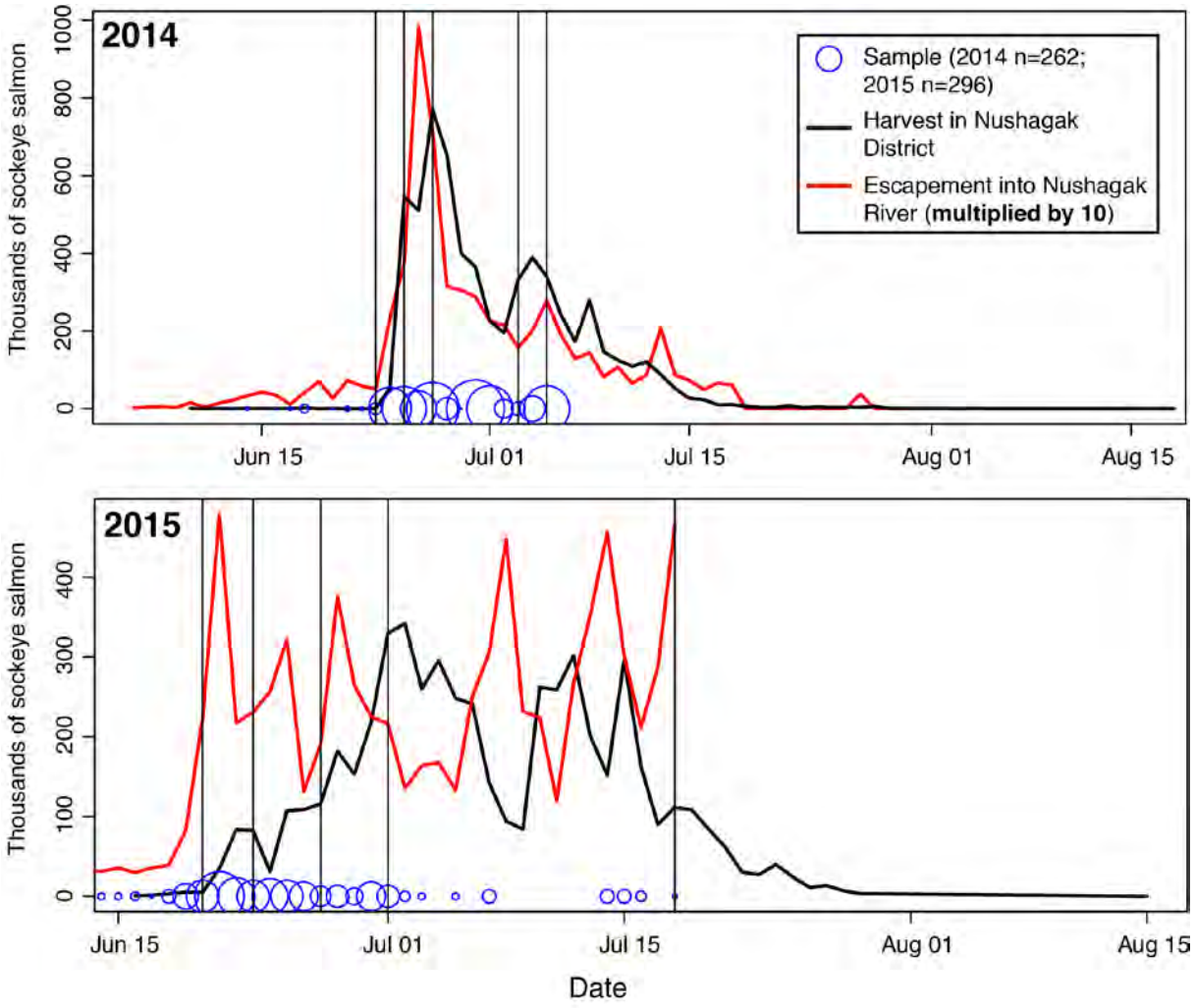

Figure 2: Strontium isoscape of the Nushagak River. Redrawn from Brennan *et al.* (2016). Habitats with the same color are characterized by the same strontium isotope ratios ($^{87}Sr/^{86}Sr$). Color groupings correspond to a range of 0.0006 in $^{87}Sr/^{86}Sr$ ratios. This represents the approximate limits of isotopic resolution when determining the natal origin of a fish based on isotopic information in its otolith. In the Nushagak, the natal origins of salmon can be assigned to habitats with distinct isotope ratios – those habitats with isotope ratios not different by more than ~0.0006 than that measured in an otolith (e.g., the distinct colors shown here).

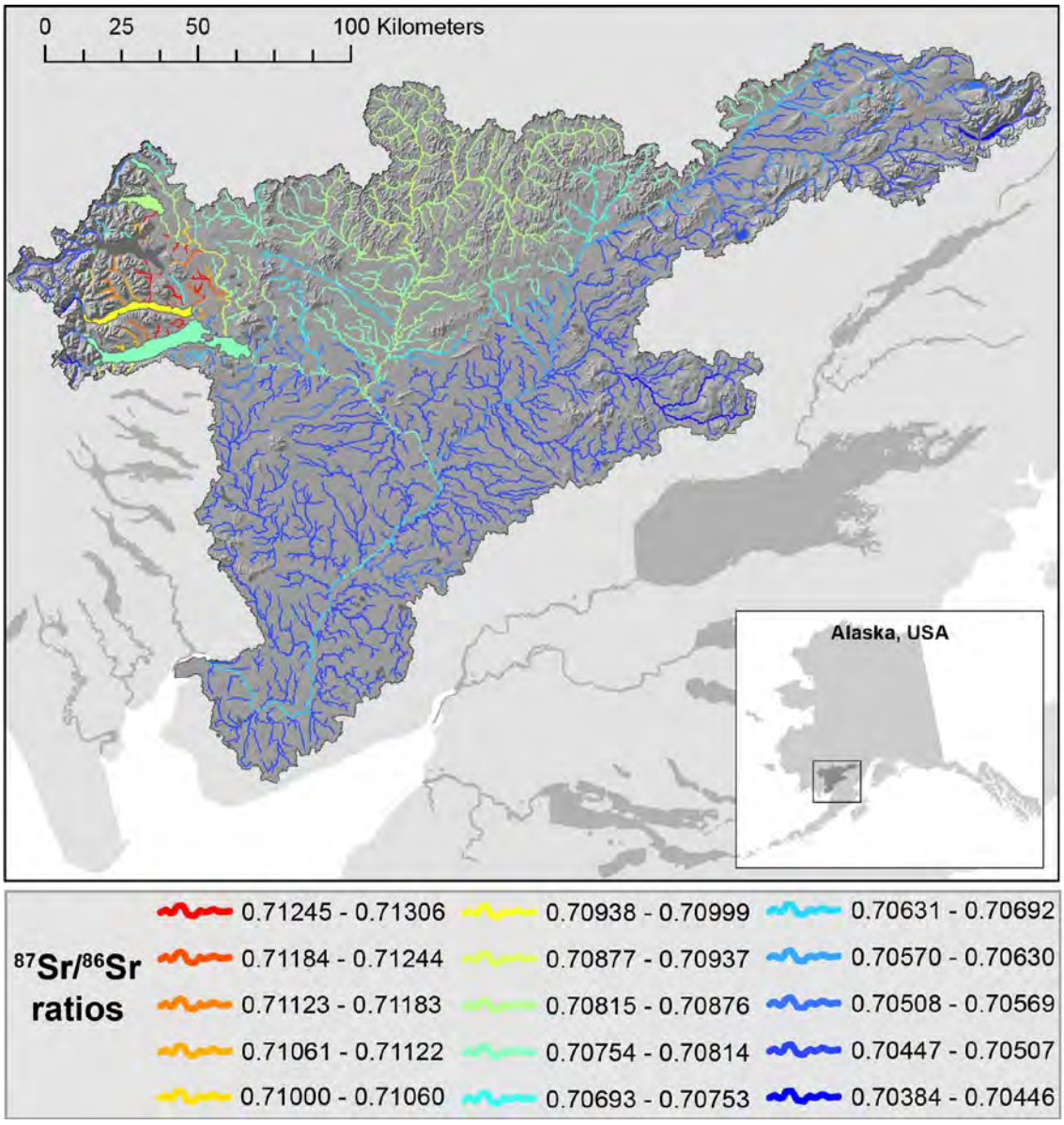

Figure 3: The relative production patterns of sockeye salmon returning to the Nushagak River in 2014.The production values have been scaled to range from 0 to 1 to ease visualization.

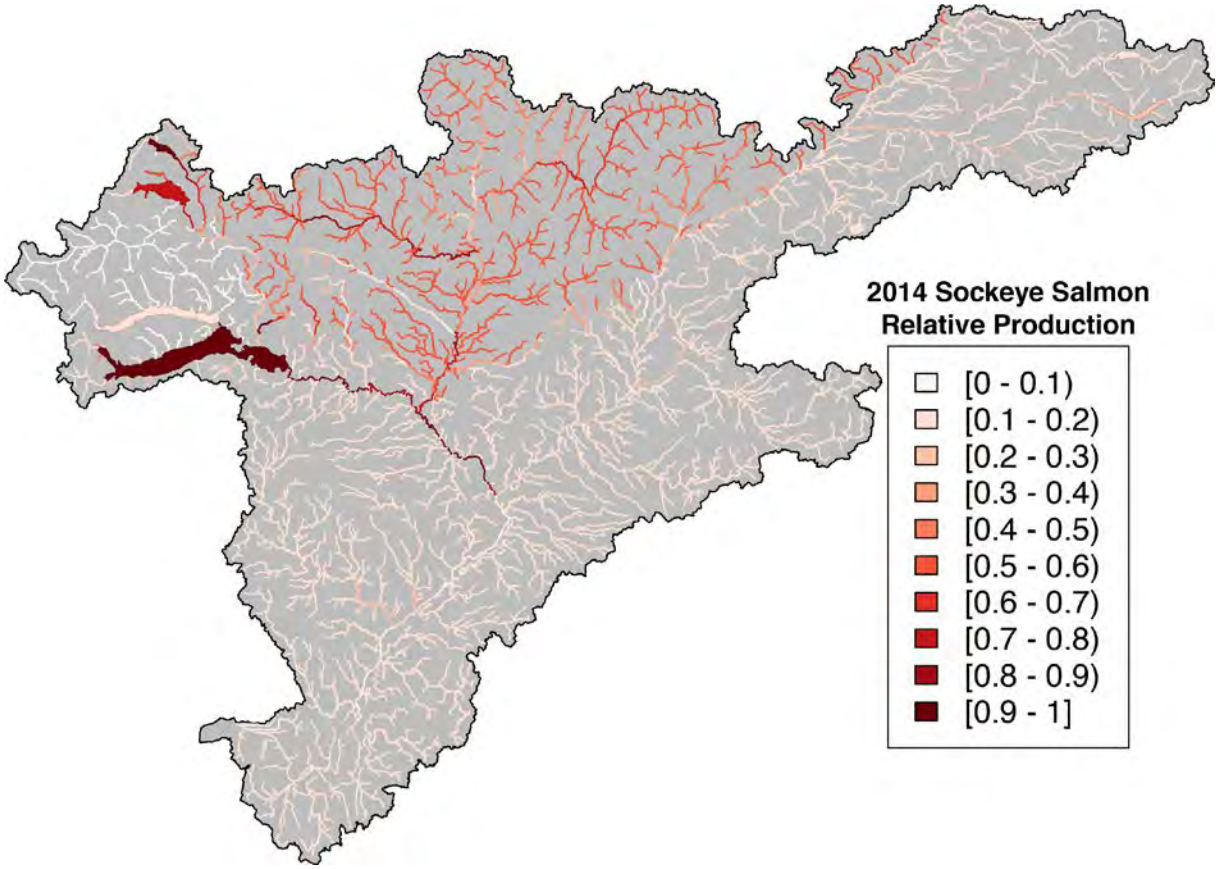

Figure 4: The relative production patterns of sockeye salmon returning to the Nushagak River in 2015.The production values have been scaled to range from 0 to 1 to ease visualization.

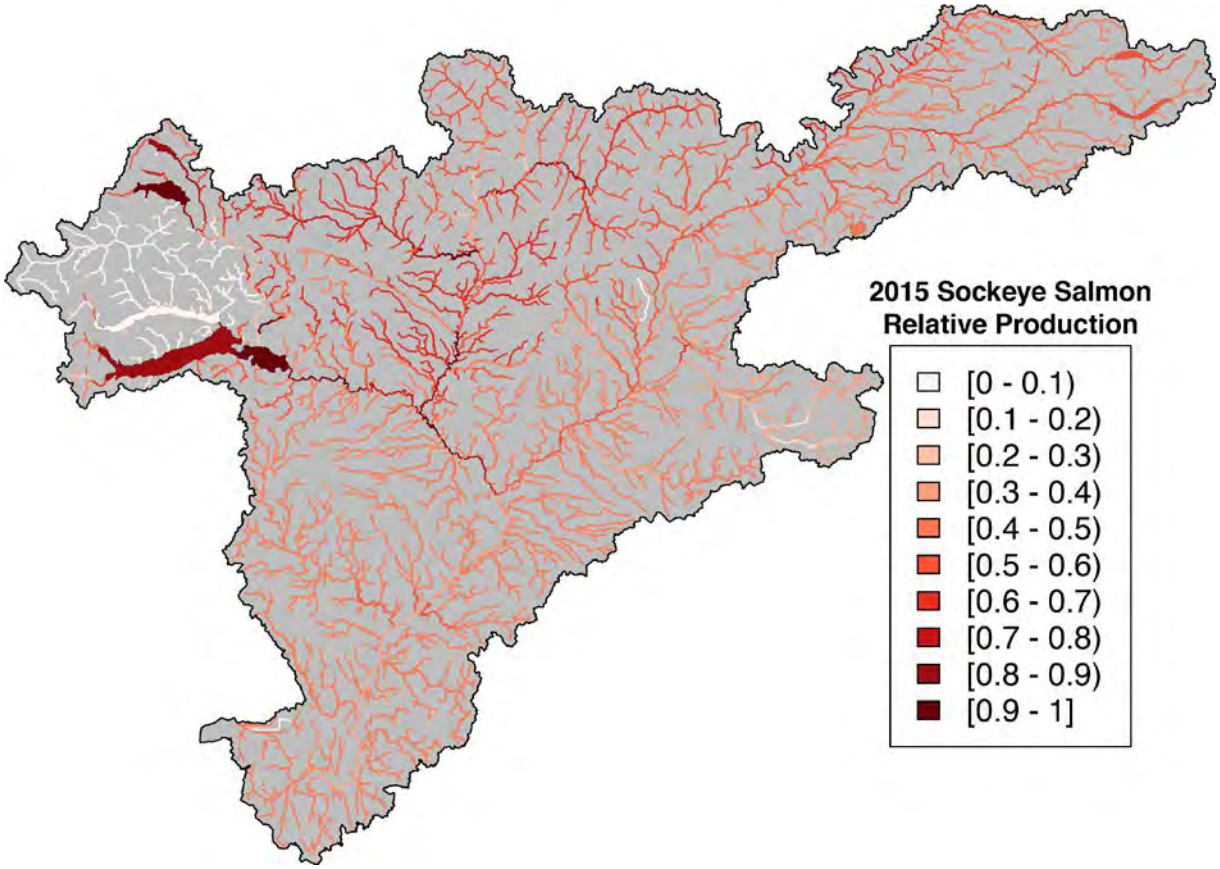

Figure 5: Production patterns of sockeye salmon that migrated to the ocean as sub-yearlings (e.g., 0.3 or 0.4 sockeye salmon) versus sockeye salmon that spent at least one year in freshwater before migrating to the ocean (e.g., 1.3 or 2.3 sockeye salmon). In 2014 and 2015, the production patterns of zero freshwater age fish (sea-type sockeye) were more diffuse throughout the basin than were patterns of sockeye salmon with freshwater ages of 1 or 2 (river- and lake-type sockeye), highlighting the importance of habitat and life history complexity in the Nushagak basin.

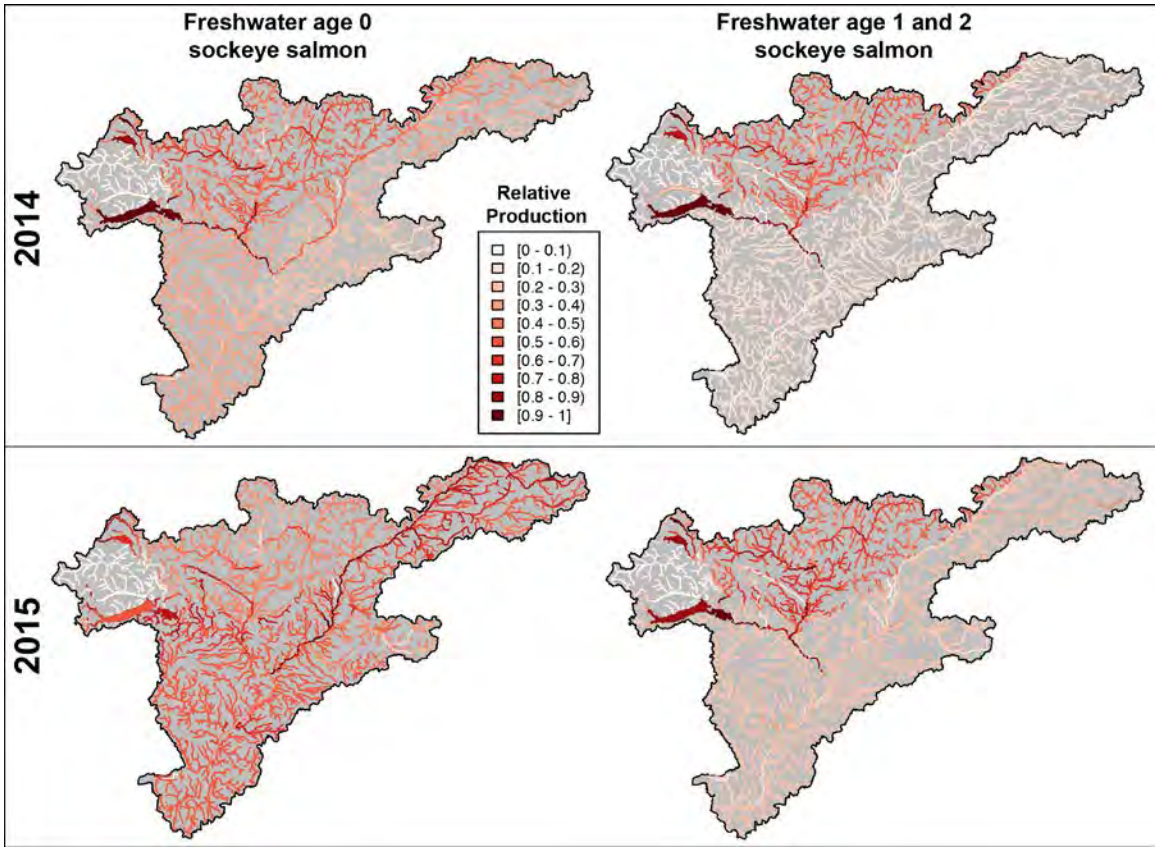

Figure 6: How production of sockeye salmon scales with the amount of available habitat. In 2014, production patterns were not particularly correlated with the amount of habitat; in 2015, the correlation was much stronger. The right panel zooms-in on the production patterns of sub basins that represent <15% of the total habitat.

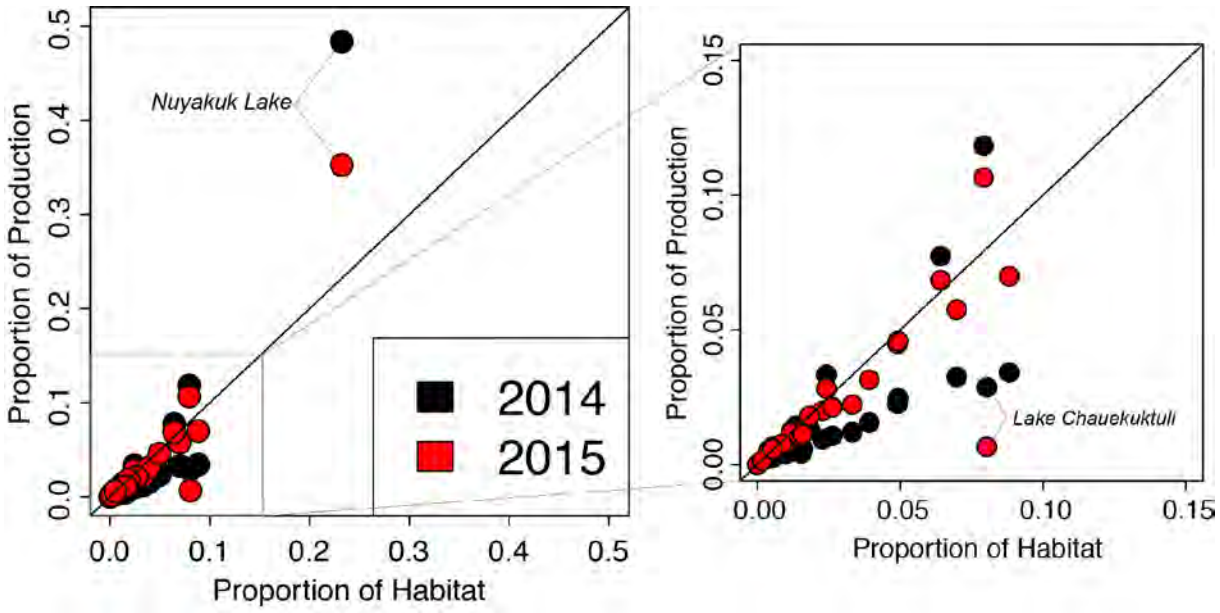

Figure 7: Age composition of the samples taken from the Portage Creek sonar site (2014 n=262; 2015 n=296 sockeye salmon).

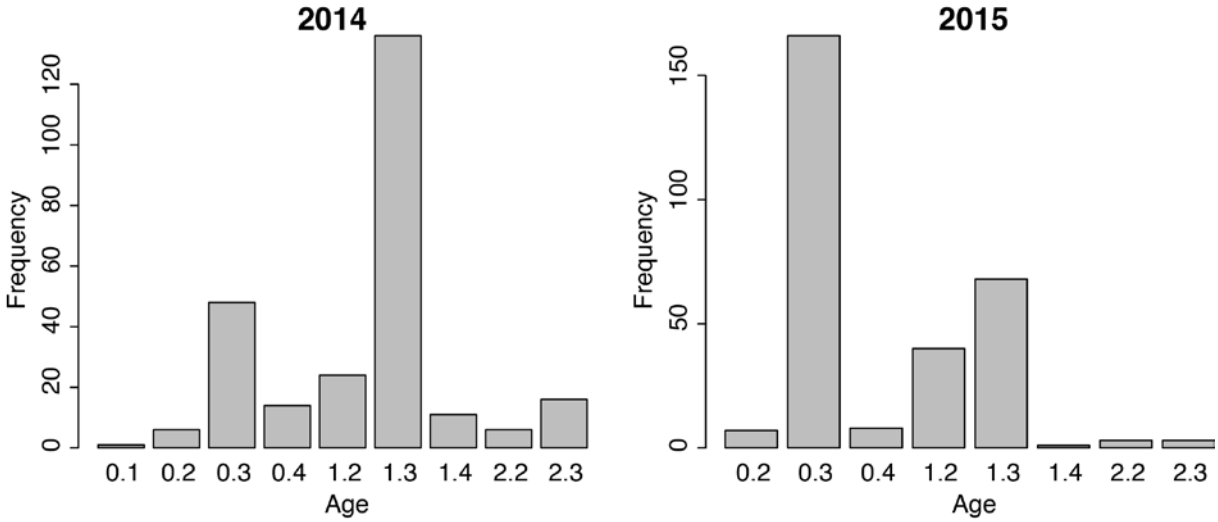

Table 1: Major tributaries throughout the Nushagak River basin and the proportion of sockeye salmon that returned in 2014 and 2015 that were produced from each of these habitats. The proportion of the Nushagak sockeye salmon habitat represented by each of these tributaries is shown for comparison. Also shown in the two colored columns is the degree to which each habitat under- or over-produced sockeye salmon based on the amount of habitat in each tributary. The last two columns show best model estimates of the total number of sockeye salmon produced from each tributary (in thousands of fish).

Nusahgak River Sub Basin	2014 Production	2015 Production	Proportion of habitat	2014 % diff from habitat	2015 % diff from habitat	Thousands of Sockeye 2014	Thousands of Sockeye 2015
Arrow	0.004	0.006	0.007	-41	-8	6.6	13.4
Chauekuktuli	0.029	0.007	0.080	-64	-92	47.4	15.1
Chichitnok	0.015	0.013	0.014	6	-8	24.0	28.6
Chikuminuk	0	0	0			0.0	0.0
Chilchitna	0.009	0.020	0.023	-59	-13	15.1	44.5
Chilikadrotna	0.022	0.045	0.049	-54	-9	35.7	101.6
Fifteenmile	0.002	0.002	0.003	-17	-25	3.5	4.5
Harris	0.004	0.005	0.006	-28	-9	7.3	12.3
Iowithla	0.004	0.009	0.011	-61	-20	6.6	19.1
KingSalmon	0.034	0.028	0.024	38	16	55.3	63.5
Klutapuk	0.003	0.003	0.003	-6	-17	5.3	6.4
Klutuk	0.004	0.008	0.010	-59	-20	6.4	17.7
Klutuspak	0.003	0.005	0.005	-52	-11	4.4	10.4
Koktuli	0.012	0.023	0.033	-64	-33	19.2	50.4
Kokwok	0.015	0.032	0.039	-60	-20	24.9	70.8
LittleKingSalmon	0.002	0.003	0.003	-18	-5	3.9	6.2
LowerRiver_mainstem_only	0.004	0.010	0.015	-73	-32	6.8	23.3
LowerRiverTribsOnly	0.033	0.070	0.088	-61	-21	54.7	156.5
MiddleNushagak_mainstem_only	0.005	0.005	0.004	33	23	8.9	11.1
MiddleNushTribsOnly	0.010	0.021	0.026	-59	-19	17.2	47.7
Mosquito	0.013	0.012	0.012	5	0	20.7	26.5
Mulchatna_mainstem	0.032	0.057	0.070	-53	-18	52.9	127.8
NuyakukLake	0.488	0.349	0.232	108	52	805.0	780.8
Nuyukak	0.013	0.018	0.018	-28	-1	21.5	40.4
OldmanCr	0.006	0.008	0.009	-33	-10	9.8	17.3
Polly	0.002	0.002	0.002	-5	-12	2.7	3.6
Stuyahok	0.006	0.011	0.016	-62	-28	9.6	25.7
Tikchik	0.118	0.108	0.079	49	34	195.4	242.8
UpperMultch	0.024	0.045	0.049	-50	-7	40.1	101.6
UpperNushagak_mainstem	0.078	0.070	0.064	21	7	128.2	155.7
Vukpalik	0.007	0.006	0.005	24	10	10.9	13.3
Total	1.000	1.000	1.000			1650.1	2238.3

** The estimates for the total number of sockeye salmon in 2014 and 2015 were provided by ADF&G's Fishery Management Reports No. 15-24 and 16-13, respectively.

References:

Bataille, C.P. & Bowen, G.J. (2012) Mapping Sr-87/Sr-86 variations in bedrock and water for large scale provenance studies. *Chemical Geology,* **304,** 39-52.

Bataille, C.P., Brennan, S.R., Hartmann, J., Moosdorf, N., Wooller, M.J. & Bowen, G.J. (2014) A geostatistical framework for predicting variations in strontium concentrations and isotope ratios in Alaskan rivers. *Chemical Geology,* **389,** 1-15.

Brennan, S.R., Fernandez, D.P., Zimmerman, C.E., Cerling, T.E., Brown, R.J. & Wooller, M.J. (2015a) Strontium isotopes in otoliths of a non-migratory fish (slimy sculpin): Implications for provenance studies. *Geochimica Et Cosmochimica Acta,* **149,** 32-45.

Brennan, S.R. & Schindler, D.E. (2017) Linking otolith microchemistry and dendritic isoscapes to map heterogeneous production of fish across river basins. *Ecological Applications,* **27,** 363-377.

Brennan, S.R., Torgersen, C.E., Hollenbeck, J.P., Fernandez, D.P., Jensen, C.K. & Schindler, D.E. (2016) Dendritic network models: Improving isoscapes and quantifying influence of landscape and in-stream processes on strontium isotopes in rivers. *Geophysical Research Letters,* **43,** 5043-5051.

Brennan, S.R., Zimmerman, C.E., Fernandez, D.P., Cerling, T.E., McPhee, M.V. & Wooller, M.J. (2015b) Strontium isotopes delineate fine-scale natal origins and migration histories of Pacific salmon. *Sci Adv,* **1,** e1400124.

Peterson, E.E. & Ver Hoef, J.M. (2010) A mixed-model moving-average approach to geostatistical modeling in stream networks. *Ecology,* **91,** 644-651.

Schindler, D.E., Armstrong, J.B. & Reed, T.E. (2015) The portfolio concept in ecology and evolution. *Frontiers in Ecology and the Environment,* **13,** 257-263.

Schindler, D.E., Hilborn, R., Chasco, B., Boatright, C.P., Quinn, T.P., Rogers, L.A. & Webster, M.S. (2010) Population diversity and the portfolio effect in an exploited species. *Nature,* **465,** 609-612.

Ver Hoef, J.M. & Peterson, E.E. (2010) A Moving Average Approach for Spatial Statistical Models of Stream Networks. *Journal of the American Statistical Association,* **105,** 6-18.

Appendix 1. Brennan SR, CE Torgersen, JP Hollenbeck, DP Fernandez, DE Schindler. 2016. Dendritic network models: improving isoscapes and quantifying influence of landscape and in-stream processes on strontium isotopes in rivers. *Geophysical Research Letters* 43: 5043-5051.

Appendix 2. Brennan SR, DE Schindler. 2017. Linking otolith microchemistry and dendritic isoscapes to map heterogeneous production of fish across river basins. *Ecological Applications* 27: 363-377.

AGU PUBLICATIONS

Geophysical Research Letters

RESEARCH LETTER
10.1002/2016GL068904

Key Points:
- Dendritic network models substantially improve isoscapes of strontium isotopes in rivers
- Models can quantify influence of landscape versus in-stream driven processes on isotopes in rivers
- Landscape and in-stream processes shape strontium isotopes in rivers at multiple spatial scales

Supporting Information:
- Supporting Information S1
- Table S1
- Table S2
- Table S3
- Table S4
- Table S5
- Table S6
- Table S7

Correspondence to:
S. R. Brennan,
srbrenn@uw.edu

Citation:
Brennan, S. R., C. E. Torgersen, J. P. Hollenbeck, D. P. Fernandez, C. K. Jensen, and D. E. Schindler (2016), Dendritic network models: Improving isoscapes and quantifying influence of landscape and in-stream processes on strontium isotopes in rivers, *Geophys. Res. Lett.*, *43*, doi:10.1002/2016GL068904.

Received 5 FEB 2016
Accepted 29 APR 2016
Accepted article online 5 MAY 2016

Dendritic network models: Improving isoscapes and quantifying influence of landscape and in-stream processes on strontium isotopes in rivers

Sean R. Brennan[1], Christian E. Torgersen[2,3], Jeff P. Hollenbeck[2], Diego P. Fernandez[4], Carrie K. Jensen[5], and Daniel E. Schindler[1]

[1]School of Aquatic and Fishery Sciences, University of Washington, Seattle, Washington, USA, [2]Forest and Rangeland Ecosystem Science Center, Cascadia Field Station, U.S. Geological Survey, Corvallis, Oregon, USA, [3]School of Environmental and Forest Sciences, University of Washington, Seattle, Washington, USA, [4]Department of Geology and Geophysics, University of Utah, Salt Lake City, Utah, USA, [5]Department of Forest Resources and Environmental Conservation, Virginia Polytechnic Institute and State University, Blacksburg, Virginia, USA

Abstract A critical challenge for the Earth sciences is to trace the transport and flux of matter within and among aquatic, terrestrial, and atmospheric systems. Robust descriptions of isotopic patterns across space and time, called "isoscapes," form the basis of a rapidly growing and wide-ranging body of research aimed at quantifying connectivity within and among Earth's systems. However, isoscapes of rivers have been limited by conventional Euclidean approaches in geostatistics and the lack of a quantitative framework to apportion the influence of processes driven by landscape features versus in-stream phenomena. Here we demonstrate how dendritic network models substantially improve the accuracy of isoscapes of strontium isotopes and partition the influence of hydrologic transport versus local geologic features on strontium isotope ratios in a large Alaska river. This work illustrates the analytical power of dendritic network models for the field of isotope biogeochemistry, particularly for provenance studies of modern and ancient animals.

1. Introduction

Isotopic tracers are used widely to quantify spatial and temporal patterns in the transport and flux of matter across Earth's surface [*Bowen*, 2010]. Such patterns provide the foundation of numerous interdisciplinary applications aiming to discern connectivity within and among aquatic, terrestrial, and atmospheric systems [*Good et al*., 2015], and the provenance, movement, and habitat use of organisms [*Hobson et al*., 2010]. The underlying framework of these applications is in robust representations of environmental isotopic variation, both with respect to sources and associated isotopic effects during transport (mixing and fractionation). Those representations have been called isoscapes or isotopic landscapes [*Bowen*, 2010].

Most isoscapes have been constructed by integrating (i) process-oriented modeling based on known mechanisms producing isotopic variation (e.g., fractionation and radioactive decay) and (ii) statistical modeling to compute the relative effects of different covariates via regression analysis and taking advantage of spatial dependencies via geostatistical interpolation. The latter is particularly important in the generation of spatially continuous estimates of isotopic variation across landscapes. Although substantial advancements have been made in the development of isoscapes, two current limitations face the field with respect to aquatic systems. First, geostatistical interpolations used to predict isotope values at unsampled locations have been limited to Euclidean space (the closest straight-line distance between two sites). Second, a quantitative framework is lacking that is able to apportion the influence of in-stream processes (e.g., downstream transport) and processes driven by connectivity to landscape features on observed isotopic patterns (e.g., aridity, vegetation cover, or geology). Spatial dependency in Euclidean space is likely adequate for modeling isoscapes of atmospheric, terrestrial, and oceanic systems, but isotopic patterns in rivers may be defined by a combination of Euclidean patterns and those dependencies unique to the dendritic networks of rivers, such as downstream transport.

A new class of geostatistical models has been developed to account for the unique spatial relationships of dendritic networks [*Peterson and Ver Hoef*, 2010; *Ver Hoef and Peterson*, 2010] and is able to apportion variance among in-stream versus landscape driven processes [*Ganio et al*., 2005; *McGuire et al*., 2014]. Unlike classical

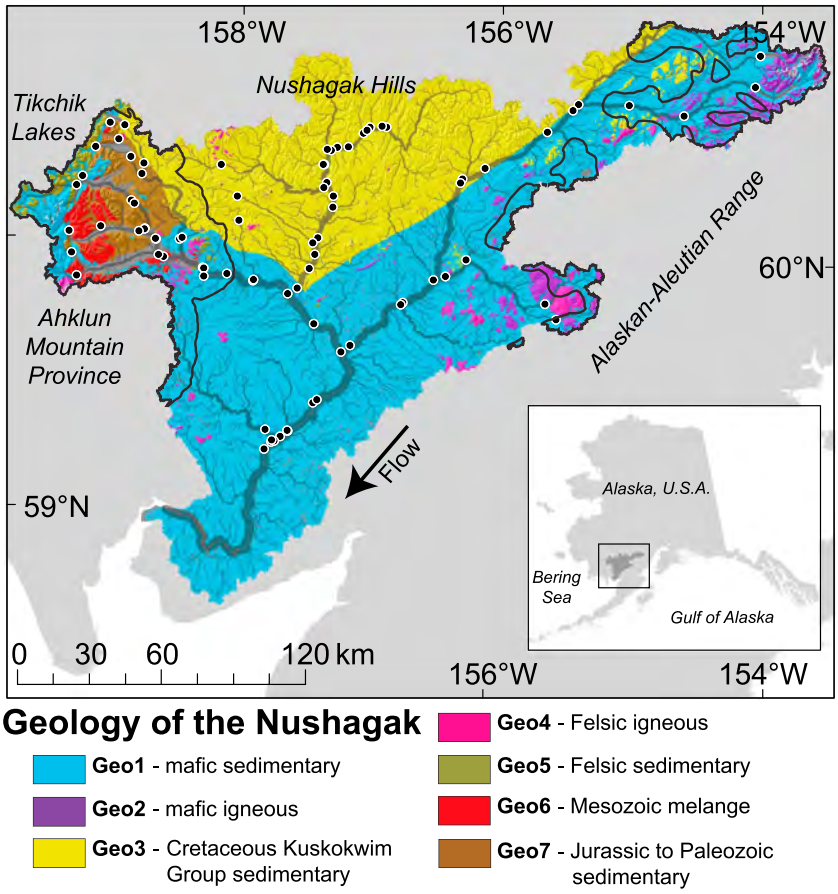

Figure 1. Geology of the Nushagak River. Black bold line indicates extent of most recent glaciation in the Nushagak basin. Black-filled circles indicate observation sites; width of streamlines is proportional to product of [Sr] and accumulated flow.

geostatistics, spatial stream network models (SSNMs) use autocovariance structures to account for the spatial dependences unique to rivers [*Isaak et al.*, 2014], such as the branching networks of streams, abrupt changes at confluences, direction of flow, and longitudinal connectivity of flowing water [*Peterson et al.*, 2013]. The application of these models to generate isoscapes of rivers has broad implications but has not yet been demonstrated. Here we show how SSNMs can be applied to improve the accuracy of riverine isoscapes and to discern the relative influence of in-stream processes versus landscape connectivity on isotopic patterns throughout rivers.

One tracer proven to be very useful in provenance and geochemical weathering research is strontium isotope ratios ($^{87}Sr/^{86}Sr$). Variation in $^{87}Sr/^{86}Sr$ has been used in a wide variety of contexts including discerning the relative influence of mantle-driven processes from continental weathering at millennia time scales on the composition of sea water [*Burke et al.*, 1982], reconstructing landscape use patterns of ancient hominids [*Copeland et al.*, 2011] and extinct megafauna [*Hoppe et al.*, 1999], and apportioning complex fishery harvests to distinct natal sources and life history strategies [*Brennan et al.*, 2015b; *Kennedy et al.*, 1997]. Current $^{87}Sr/^{86}Sr$ isoscapes [*Bataille et al.*, 2014] perform well at large continental spatial scales and at reproducing general patterns but poorly in geologically complex areas (e.g., metasedimentary regions). Their uncertainty is also relatively high ($\geq$0.0015) compared to the resolution relevant for many provenance applications (e.g., 0.0004 in *Brennan et al.* [2015b]). Improving the accuracy of $^{87}Sr/^{86}Sr$ river isoscapes, thus, has broad implications for provenance and geochemical weathering research.

To demonstrate the application of SSNMs for developing isoscapes and quantifying landscape versus in-stream driven processes on isotopic patterns in rivers, we applied these models to $^{87}Sr/^{86}Sr$ ratios in water throughout the Nushagak River in southwestern Alaska (Figure 1). $^{87}Sr/^{86}Sr$ ratios were temporally stable at subannual and interannual time scales within this watershed [*Brennan et al.*, 2015a], thus simplifying any interpretation of spatial patterns. We expected SSNMs to improve accuracy of predictions and that landscape features

would play a dominant role in shaping isotopic patterns (i.e., geologic heterogeneity) but would be modified by longitudinal transport as Sr is routed downstream through the network.

2. Materials and Methods

Estimating $^{87}Sr/^{86}Sr$ ratios in surface waters throughout the Nushagak River using SSNMs required (i) synthesizing multiple geospatial data products (Text S1 in the supporting information), including geologic maps, a digital elevation model (DEM), a network topology free of geometric errors, and measured $^{87}Sr/^{86}Sr$ and strontium concentrations (mg/L, referred to hereafter as [Sr]) values throughout the network, (ii) an SSNM of [Sr] throughout the network, (iii) an SSNM of $^{87}Sr/^{86}Sr$ ratios which incorporated the results from the model of [Sr] in the form of a spatial weighting scheme, (iv) identifying the best performing models, and (v) using this model to estimate $^{87}Sr/^{86}Sr$ ratios for each stream segment within the river network. All data analyses were conducted in R (http://cran.r-project.org/) using the Spatial Stream Network (SSN) package [*Ver Hoef et al*., 2014] and Spatial Tools for the Analysis of River Systems (STARS) toolbox in ArcGIS 10.2 [*Peterson and Ver Hoef*, 2014].

2.1. Spatial Linear Mixed Models

We used SSNMs to analyze a published water data set [*Brennan et al*., 2015a], with additional data (total $n = 86$ sites) describing $^{87}Sr/^{86}Sr$ ratios throughout the Nushagak River (Figure 1). Complete formulations of these models are described elsewhere [*Peterson and Ver Hoef*, 2010; *Ver Hoef and Peterson*, 2010]. Briefly, SSNMs use a moving average (MA) construction based on hydrologic distance, which is the shortest distance between any two points measured along the stream network. The branching nature of river systems requires the MA functions to split at stream junctions, and this is done by using spatial weighting schemes based on watershed features, such as upstream area or volume of flow. By using a mixed-effects modeling framework, SSNMs are able to account for the variance explained by a set of covariates as fixed effects (e.g., percent geology type) and the variance explained by different autocovariance functions as random effects. In addition to Euclidean autocorrelation, SSNMs can explicitly quantify the spatial dependence between flow-connected and flow-unconnected sites via "tail-up" and "tail-down" autocovariance structures, respectively [*Ver Hoef and Peterson*, 2010]. Tail-up models account for autocorrelation among flow-connected sites in an upstream direction. Tail-down models account for autocorrelation among flow-connected and flow-unconnected sites in a downstream direction. The general form of these spatial linear mixed models is

$$\mathbf{y} = \mathbf{X}\boldsymbol{\beta} + \mathbf{z}_{TU} + \mathbf{z}_{TD} + \mathbf{z}_{E} + \boldsymbol{\varepsilon}, \tag{1}$$

where $\mathbf{y}$ is the vector of the response variable ($^{87}Sr/^{86}Sr$ ratios or [Sr]), $\mathbf{X}$ is a matrix of covariates (e.g., percent geology types), $\boldsymbol{\beta}$ is a vector of the parameters for each covariate, $\mathbf{z}_{TU}$, $\mathbf{z}_{TD}$, and $\mathbf{z}_{E}$ are vectors of random variables with tail-up, tail-down, and Euclidean correlation structures, respectively, and $\boldsymbol{\varepsilon}$ is a vector of independent random errors.

2.2. Spatial Weights

SSNMs require spatial weights computed along the stream network to inform how the MA functions split at stream junctions. SSNMs use "segment proportional influence" to compute the relative influence of each stream segment on its downstream segment. A "segment" corresponds to the length of stream between two junctions within a river network. For example, if q denotes some watershed quantity measured at all segments, such as upstream area, and i and j are segments flowing into segment k, then SSNMs compute weights, ω_i, as $\omega_i = q_i/(q_i + q_j)$, and $\omega_j = q_j/(q_j + q_i)$ where $\omega_i + \omega_j = 1$, such that ω_i and ω_j denote the proportional influence of segments i and j on k based on upstream area. Commonly, SSNM spatial weights are based on watershed area. Other weighting schemes include using estimates of stream flow. As a proxy for flow, we used a gridded estimate of the decadal mean annual precipitation amount (mm) throughout the entire basin (Text S1) and accumulated these estimates at each river segment using the STARS toolbox in ArcGIS [*Peterson and Ver Hoef*, 2014]. In addition to the amount of water flowing past any location within the network, the reactivity of different geologic materials (e.g., carbonate minerals versus silicates) influence how much Sr is released into rivers. As such, we combined estimates of the precipitation and [Sr] in river water into one spatial weight defined as the product of these two parameters (Figure 1). Thus, to estimate $^{87}Sr/^{86}Sr$ ratios throughout the entire Nushagak River, we first used SSNMs to estimate [Sr] values throughout the network using precipitation to compute weights. We then used these estimates to calculate the spatial weights for

the $^{87}Sr/^{86}Sr$ model, defined as the product of [Sr] and precipitation from all upstream components of the watershed at a given site.

2.3. Predictors

To make this approach transferrable among systems, we used a set of simple covariates as predictors of $^{87}Sr/^{86}Sr$ ratios derived from commonly available geospatial data products (Table S1). The geology of the Nushagak basin was simplified into seven major groups based on lithology type and age (Figure 1 and Text S1). The percent area was computed for each lithological group contributing to all downstream locations throughout the catchment. Here these locations included "prediction sites" (the midpoint of each unique stream segment) and "observation sites" (Figure 1). Using the mixed-effects framework of SSNMs we fit equation (1) using observation sites. We compared multiple candidate models differing in fixed effects and autocovariance functions using AIC (Akaike information criterion: a measure of model performance by balancing trade-offs between overfitting and complexity). Multiple types of autocovariance functions for each spatial relationship were tested (e.g., exponential, spherical, and linear sill) available in the SSN R package [*Ver Hoef et al*., 2014]. After identifying the best model via AIC, we then estimated $^{87}Sr/^{86}Sr$ ratios at each prediction-site throughout the network.

To develop an SSNM for [Sr] throughout the Nushagak River, we tested additional predictors also known to influence geochemical weathering including relief and the watershed area recently glaciated (Table S1). We estimated relief using multiple metrics including percent slope and "local relief," which we define as the difference between the maximum and minimum elevations within each reach contributing area—the local basin area that contributes to each segment within the network. To evaluate the effect of recent glaciations, we computed the percent area upstream of each segment that was glaciated during the Late Wisconsin (Figure 1) [*Manley and Kaufman*, 2002].

2.4. Empirical Semivariograms

We used empirical semivariograms (ES), which describe spatial structure in [Sr] and $^{87}Sr/^{86}Sr$ ratios by calculating the semivariance (γ of observations as a function of distance (d), to analyze patterns in flow-connected, flow-unconnected, and Euclidean spatial relationships. ESs of the former two are referred to as Torgegrams, which illustrate the $\gamma(d)$ of each network relationship separately [*Peterson et al*., 2013]. Semivariance was calculated using the robust estimator of *Cressie* [1993] (as in *Ganio et al*. [2005]) and a lag class interval of 15 km; calculations of γ were based on $\geq$30 pairs of sample points [*Rossi et al*., 1992]. Torgegrams were evaluated visually based on the methods of *McGuire et al*. [2014] to identify broad scale, fine scale, or nested scales of heterogeneity in [Sr] and $^{87}Sr/^{86}Sr$ ratios.

2.5. Water Analyses

The additional water samples reported here ($n = 20$ sites) were collected, filtered, and acidified as in *Brennan et al*. [2014]. These samples came from the Tikchik Lakes region (Figure 1), a geologically complex area with the oldest and most chemically reactive (marine limestone) lithologies in the basin (Table S2). Water samples were analyzed for [Sr] and $^{87}Sr/^{86}Sr$ ratios using single and multicollector inductively coupled plasma mass spectrometry (Text S1).

3. Results

$^{87}Sr/^{86}Sr$ ratios from the 20 new sites ranged from 0.70477 to 0.71163 (Table S3), a 50% increase in the range of observed $^{87}Sr/^{86}Sr$ ratios in the Nushagak River basin [*Brennan et al*., 2015a]. [Sr] ranged from 0.0220 to 0.1462 mg/L; [Sr] in the field blank was below the limit of detection ($<$0.00003 mg/L). Standard deviations (2SD) of $^{87}Sr/^{86}Sr$ ratios and [Sr] of the field triplicate were ±0.00002 and ±0.0003 mg/L (King Salmon River), respectively, which is consistent with previous work in this watershed [*Brennan et al*., 2015a].

3.1. Multiscale Spatial Structure of $^{87}Sr/^{86}Sr$ and [Sr] Within the Nushagak

$^{87}Sr/^{86}Sr$ ratios and [Sr] showed multiscale spatial structure with respect to flow-connected, flow-unconnected, and Euclidean relationships (Figure 2). Torgegrams for both tracers showed evidence of fine-scale structure at $<$50–85 km, as indicated by consistent inflection points in γ at these distances; the fine-scale inflection points for flow-unconnected and Euclidean were more subtle for $^{87}Sr/^{86}Sr$ ratios. Flow-unconnected and Euclidean semivariograms also exhibited consistently higher and more variable γ

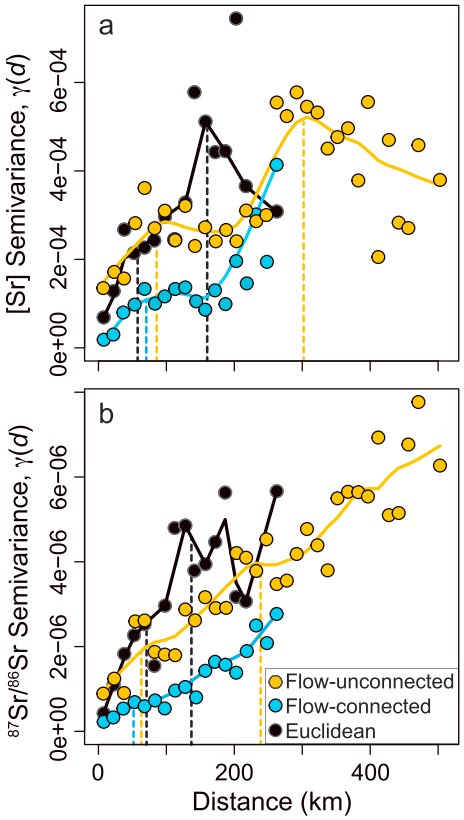

Figure 2. Semivariograms of (a) [Sr] and (b) $^{87}Sr/^{86}Sr$ ratios for the Nushagak basin, indicating nested spatial structure for flow-unconnected, flow-connected, and Euclidean relationships. Vertical dotted lines indicate fine- and broad-scale ranges visually determined by inflection points. Solid lines were smoothed to data using LOWESS (locally weighted scatterplot smoothing; smoothing factor = 1/3).

compared to flow-connected sites, especially at distances >150 km. Broad-scale spatial structure in [Sr] and $^{87}Sr/^{86}Sr$ was more variable, persisting to distances of 150 km for Euclidean relationships and >250 km for flow-connected and flow-unconnected relationships. These ranges also corresponded well with patch sizes for the geologic groups considered here (Table S1).

3.2. Model Results

The distribution of [Sr] exhibited positive skew, so data were log transformed before fitting models. The best model for predicting [Sr] throughout the Nushagak River included all geology types (Geo1–7), local relief, and the extent of the most recent glaciation as fixed effects (Figure 3a and Table S4). As random effects, this model included Epanechnikov tail-up [*Garreta et al.*, 2010] and Gaussian Euclidean autocovariance functions. Of all the models tested, the nonspatial model performed most poorly (ΔAIC = 70.9, the difference in AIC between a candidate model and the best model) and the model including only Euclidean autocovariance was also one of the lowest ranked (ΔAIC = 49.2). In the best model, the fixed effects explained 42.0% of variation (r^2) in [Sr], while the tail-up and Euclidean autocorrelation functions explained 38.7% and 17.5% of the variation, respectively (Table S5).

The best model for predicting $^{87}Sr/^{86}Sr$ ratios across the Nushagak River included three geology types (Table S6), $Geo3_{Kk}$, $Geo6_{Mzm}$, and $Geo7_{JPz\_carb\_seds}$ (Figure 3b). As random effects, it included Epanechnikov tail-up and exponential tail-down autocovariance functions. As with the [Sr] model, the nonspatial $^{87}Sr/^{86}Sr$ model performed the worst (ΔAIC = 51.6), and a model including only Euclidean autocovariance also performed poorly (ΔAIC = 48.9) (Table S6). In the best model, the fixed effects explained 70.5% of the variation in $^{87}Sr/^{86}Sr$, while the tail-up and tail-down autocorrelation models explained 22.9% and 4.4%, respectively (Table S7). Using leave-one-out cross validation, the root-mean-square prediction error (RMSPE) of the best model was 0.00051, and the r^2 of modeled versus observed ratios was 0.90 (Figure S1). The standard error (SE) of all predictions across the network ranged from 0.0002 to 0.0012 (Figure S2).

4. Discussion and Conclusions

By explicitly modeling the unique spatial structure of rivers, we generated an $^{87}Sr/^{86}Sr$ isocape that produced excellent fit to observations distributed throughout the watershed (RMSPE = 0.00051). We also identified multiscale spatial patterns of [Sr] and $^{87}Sr/^{86}Sr$ ratios in rivers via flow-connected, flow-unconnected, and Euclidean relationships, indicating interactive effects of landscape and in-stream processes on these constituents.

4.1. In-Stream and Landscape Processes Shape [Sr] and $^{87}Sr/^{86}Sr$ Ratios in Rivers

Flow-connected, flow-unconnected, and Euclidean relationships of $^{87}Sr/^{86}Sr$ ratios and [Sr] all exhibited nested spatial structure, where both broad-scale and fine-scale processes influenced these constituents

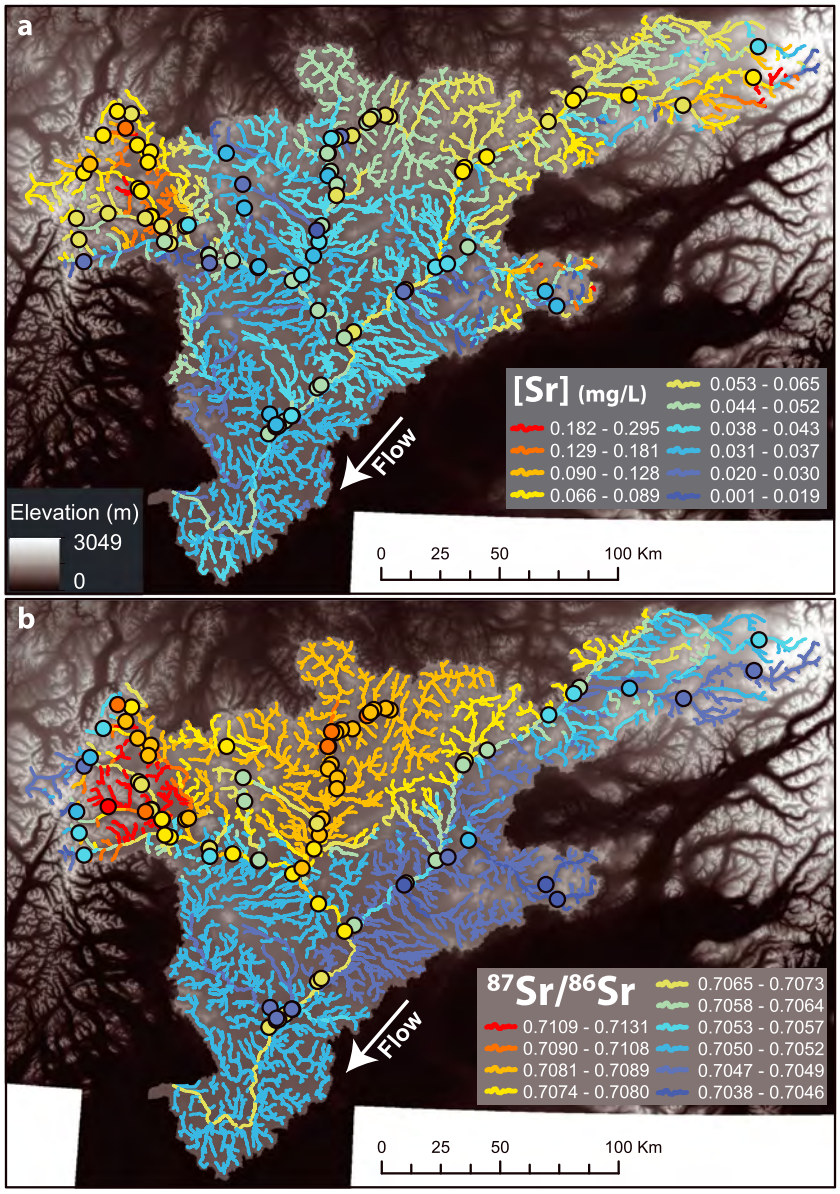

Figure 3. Predicted (a) [Sr] and (b) $^{87}Sr/^{86}Sr$ ratios across the Nushagak River. Colored circles indicate observations; colors of both circles and streams use the same breaks (natural breaks in data set; intervals > SE of prediction).

[*McGuire et al*., 2014]. Inspection of ESs provided insights into the degree of control by landscape and in-stream processes on observed patterns (Figure 2). Flow-connected relationships may indicate in-stream driven processes, i.e., longitudinal connectivity via downstream transport, whereas flow-unconnected and Euclidean relationships may reflect the influence of landscape features, including geology. Here flow connections consistently yielded lower variance as a function of distance compared to the other spatial relationships, illustrating the strong influence of longitudinal transport on $^{87}Sr/^{86}Sr$ and [Sr]. Strong coherence at fine spatial scales in the flow-unconnected and Euclidean semivariograms (Figure 2), and their similarly nested profiles, illustrates the influence of geologic heterogeneity across the landscape. The fine-scale structure, in the Torgegrams (<50–85 km), likely reflects abrupt changes occurring at stream confluences and geologic boundaries (faults). The large areas, or "patch sizes" (Table S1), of some geologic units likely drive broad-scale patterns. Thus, isotopic homogeneity is characteristic within units, which can correspond to broad ranges, whereas isotopic heterogeneity defines areas proximate to geologic boundaries at fine scales and at broad scales between discrete lithological units with large patch sizes.

The best $^{87}Sr/^{86}Sr$ model indicated that landscape processes explained 75% (fixed effects + tail down) of the variation, while 23% (tail up) was accounted for by longitudinal connectivity via hydrological transport. Incorporating Euclidean autocovariance did not improve the model, suggesting that the covariates of geology type accounted for Euclidean patterns. The tail-down autocovariance (explaining 4%) is likely due to similarities in landscape features located upstream of confluences sharing similar geology (range $<$ 150 km, Figure S3). Longitudinal connectivity explained the majority of the variance not explained by fixed effects (23%), reflecting the process of downstream routing of Sr through the river network and the mixing of isotopically different tributaries into higher-order reaches.

Landscape processes (fixed effects + Euclidean) explained less variation in the [Sr] model (60%) compared to the $^{87}Sr/^{86}Sr$ model, while longitudinal connectivity explained the remainder (tail up = 39%). The fact that fixed effects alone only explained 42%, while Euclidean patterns absorbed an additional 18%, suggests that geology-type, relief, and recent glaciation history were not sufficient at explaining all the landscape processes influencing spatial variation in [Sr]. Possible landscape features affecting [Sr] could be differences in the temperature effect on chemical weathering across the basin or vegetation cover via documented effects of interspecific differences on Sr cycling in boreal forests [*Poszwa et al*., 2004]. Nonetheless, the flexible mixed modeling framework of the SSNM was able to account for this variation by including Euclidean autocovariance. Similar to the isotope model, longitudinal connectivity was an important process shaping [Sr], explaining 39% of the variation.

4.2. SSNMs Improve Predictions of [Sr] and $^{87}Sr/^{86}Sr$ Ratios in Rivers

The RMSPE of the best $^{87}Sr/^{86}Sr$ model was almost an order of magnitude smaller than the process-oriented approach of *Bataille et al*. [2014] (RMSPE = 0.0045; if excluding four outliers = 0.0015). Comparing the *Bataille et al*. [2014] model to the SSNMs here requires caution, as the two models differ in spatial scale and also in the nature of their target predictions (prediction of each grid cell as in *Bataille et al*. [2014] versus each river segment within a network via SSNMs). However, metrics such as r^2 and RMSPE of their cross-validation tests provide some insight into the relative performance of these approaches, both of which show marked improvements for the SSNMs (Figure S1 and Tables 3 and 4) [*Bataille et al*., 2014]. Although caution is required when comparing cross-validation tests, from a modeling process standpoint, the SSNMs here also point out the advantages of accounting for the dendritic spatial structure of rivers and of making predictions at the level of stream segments versus grid cells when the goal is to analyze isotopic patterns throughout rivers.

To date, the general approach for generating $^{87}Sr/^{86}Sr$ isoscapes has been to estimate isotopic values at the "local" level (1 km grid cells) using a mixture of process-oriented and statistical methods and then to apply a flow accumulation model to represent values along a river network [*Bataille and Bowen*, 2012; *Bataille et al*., 2014]. To estimate local values, these efforts integrate bedrock geology and chemical weathering models. $^{87}Sr/^{86}Sr$ ratios of bedrock are estimated as a function of rock age, rock type, and also the recycling history of siliclastic sediments during the tectonic evolution of geologic terranes [*Bataille et al*., 2014]. The only statistical aspects of this formulation are the geostatistical interpolations used to compute the needed parameters for the $^{87}Sr/^{86}Sr$ evolution equations of bedrock at all locations. The chemical weathering portion of the *Bataille et al*. [2014] model is primarily statistical, using a multiple regression to predict [Sr] at all locations as a function of lithology type and other parameters, such as slope and permafrost. To represent the isotopic composition of river networks, a flow accumulation model is then applied to these local estimates using a DEM and gridded estimates of precipitation via ArcGIS's "Flow Accumulation" tool (Spatial Analyst Toolbox) [*Bataille et al*., 2014].

Implicit in such approaches is that the model accurately predicts local isotope values and there is no modification of isotope values during transport. Although the latter may be valid for conservative constituents such as [Sr] and $^{87}Sr/^{86}Sr$, the former is likely not valid at all locations. In primarily igneous terranes, predictions of $^{87}Sr/^{86}Sr$ perform well, due to accurate dating techniques and the known half-life of ^{87}Rb. However, sedimentary and metamorphic processes, which reconstitute and mix multiple source rock materials, pose difficult challenges to process-oriented approaches, as is evident by significant reductions in performance of sedimentary bedrock models [*Bataille and Bowen*, 2012; *Bataille et al*., 2014] and the significant deviations of river water predictions in metamorphic regions [*Bataille et al*., 2014].

The primarily statistical approach of SSNMs outlined here allows predictions of stream segments to be based on known drivers of isotopic variation (bedrock heterogeneity and differential chemical weathering), but not restricted by deterministic estimates at each local grid cell. Thus, in SSNMs the effects of covariates are calibrated to regional and local conditions and what is not explained by covariates can be incorporated via different spatial autocovariance functions. The importance of network and Euclidean spatial structure is particularly evident in the ESs of both tracers after the fixed effects have been fit to the data (Figure S3), all of which show spatial dependence. Furthermore, the utility of SSNMs is not limited to solely generating isoscapes. Rather, SSNMs also yield unique insights into the elusive interplay between in-stream and landscape processes driving isotopic patterns in rivers.

The limitations of the SSNM approach include the need for a spatially representative data set and a topologically correct network. The SE of predictions from SSNMs are sensitive to the sampling distribution throughout a study region, where extrapolation yields larger errors than interpolation (Figure S2). Thus, it is important to obtain observations in both headwater and downstream regions. Provenance and geochemical weathering studies, however, require sampling surveys that span the topological and geological variation expressed across watersheds. As the use of SSNMs grows, and improvements to hydrography data sets and DEMs accumulate, topologically correct networks will be easier to obtain. Coupling SSNMs with process-oriented approaches should lead to better predictions and insights into isotopic patterns at fine to continental scales.

4.3. Implications for Other Isotope Systems

SSNMs have broad implications for the analysis and prediction of spatial patterns of other isotope systems in rivers. For example, similar to the more process-oriented $^{87}Sr/^{86}Sr$ isoscapes, the best performing δ^2H and $\delta^{18}O$ river isoscapes apply a flow accumulation model to gridded estimates of precipitation isotope values [*Bowen et al*., 2011]. However, the same implicit assumptions apply because these model formulations assume that local predictions are accurate and there is no isotopic modification during transport. For the stable isotope systems of $^2H/^1H$ and $^{18}O/^{16}O$, these assumptions are not likely met, particularly the latter at all locations along a flow path. River isoscapes of δ^2H and $\delta^{18}O$ generated using flow accumulation models perform quite well, but they also exhibit systematic biases in predictions. These biases may be due to evaporative effects on the isotopic composition of waters during transport or to the relative influence of transpiration across basins [*Bowen et al*., 2011]. SSNMs provide a viable framework to quantify these effects separately. Furthermore, final isoscape surfaces produced via these formulations incorporate a "residual correction" step, whereby a Euclidean geostatistical model is used to interpolate between observed residuals, which are subtracted from the original model. Because SSNMs account for flow-connected and flow-unconnected spatial dependencies of river networks, their predictions will likely be more accurate than nonspatial models or those based solely on Euclidean distance (Tables S4 and S6). SSNMs may minimize the need for circular residual corrections, or if needed, will make the interpolated residual surface more accurate by accounting for network relationships.

4.4. Implications for Provenance Studies

The ability to generate accurate $^{87}Sr/^{86}Sr$ isoscapes has important implications for provenance research. The uncertainty of current Sr isoscapes [*Bataille et al*. [2014]] represents an isotopic range potentially meaningful to a variety of provenance investigations. For example, $^{87}Sr/^{86}Sr$ ratios were used to assign adult Chinook salmon caught in a coastal fishery back to seven natal regions in the Nushagak River; the 2SD of each natal region was ±0.0004 [*Brennan et al*., 2015b]. Further, nearly 50% of the Earth's surface, and 70% of Alaska's, is composed of siliclastic sedimentary rocks [*Hartmann and Moosdorf*, 2012]. Because current process-oriented models indicate reduced performance in these geologically complex regions, application of SSNMs in these areas will refine applications of isoscapes to provenance research. For example, the eastern interior of Alaska is defined by metasedimentary lithologies, where predicted river $^{87}Sr/^{86}Sr$ ratios exhibit large deviations from observed [*Bataille et al*., 2014]. Interior Alaska supports several species of Pacific salmon and was also ice free during the last glaciation, providing important refugia for ancient humans [*Potter et al*., 2011] and extinct megafauna [*Guthrie*, 2006]. The radiogenic composition of the eastern interior defines a strong east-west isotopic gradient within this corridor. Accurately characterizing such a gradient will provide a viable framework to discern migrations of ancient and modern animal populations.

Acknowledgments
The Bristol Bay Regional Seafood Association and Bristol Bay Science Research Institute funded this research. Alaska Sea grant R/100-02 funded non-Tikchik Lake [Sr] analyses. Thanks to Christine Woll and the Alaska Chapter of The Nature Conservancy for work on the Nushagak River topology; Erin Peterson, Jay Ver Hoef, Daniel Isaak, Jeff Falke, and David Hockman-Wert for training in STARS/SSN; Gabriel Bowen and the SPATIAL Short Course faculty at the University of Utah for training and financial support of SRB to attend course; Adrianne Smits for help with fieldwork; Clement Bataille for his helpful discussions; two anonymous reviewers and Christian Zimmerman. Any use of trade, product, or firm names is for descriptive purposes only and does not imply endorsement by the U.S. government. Data used are listed in the supporting information.

References

Bataille, C. P., and G. J. Bowen (2012), Mapping Sr-87/Sr-86 variations in bedrock and water for large scale provenance studies, *Chem. Geol.*, *304*, 39–52.

Bataille, C. P., S. R. Brennan, J. Hartmann, N. Moosdorf, M. J. Wooller, and G. J. Bowen (2014), A geostatistical framework for predicting variations in strontium concentrations and isotope ratios in Alaskan rivers, *Chem. Geol.*, *389*, 1–15.

Bowen, G. J. (2010), Isoscapes: Spatial pattern in isotopic biogeochemistry, *Annu. Rev. Earth Planet. Sci.*, *38*(38), 161–187.

Bowen, G. J., C. D. Kennedy, Z. F. Liu, and J. Stalker (2011), Water balance model for mean annual hydrogen and oxygen isotope distributions in surface waters of the contiguous United States, *J. Geophys. Res.*, *116*, G04011, doi:10.1029/2010JG001581.

Brennan, S. R., D. P. Fernandez, G. Mackey, T. E. Cerling, C. P. Bataille, G. J. Bowen, and M. J. Wooller (2014), Strontium isotope variation and carbonate versus silicate weathering in rivers from across Alaska: Implications for provenance studies, *Chem. Geol.*, *389*, 167–181.

Brennan, S. R., D. P. Fernandez, C. E. Zimmerman, T. E. Cerling, R. J. Brown, and M. J. Wooller (2015a), Strontium isotopes in otoliths of a non-migratory fish (slimy sculpin): Implications for provenance studies, *Geochim. Cosmochim. Acta*, *149*, 32–45.

Brennan, S. R., C. E. Zimmerman, D. P. Fernandez, T. E. Cerling, M. V. McPhee, and M. J. Wooller (2015b), Strontium isotopes delineate fine-scale natal origins and migration histories of Pacific salmon, *Sci. Adv.*, *1*(4e1400124), doi:10.1126/sciadv.1400124.

Burke, W. H., R. E. Denison, E. A. Hetherington, R. B. Koepnick, H. F. Nelson, and J. B. Otto (1982), Variation of seawater $^{87}Sr/^{86}Sr$ throughout Phanerozoic time, *Geology*, *10*, 516–519.

Copeland, S. R., M. Sponheimer, D. J. de Ruiter, J. A. Lee-Thorp, D. Codron, P. J. le Roux, V. Grimes, and M. P. Richards (2011), Strontium isotope evidence for landscape use by early hominins, *Nature*, *474*(7349), 76–78, doi:10.1038/nature10149.

Cressie, N. A. C. (1993), *Statistics for Spatial Data*, Rev. ed., 900 pp., Wiley, New York.

Ganio, L. M., C. E. Torgersen, and R. E. Gresswell (2005), A geostatistical approach for describing spatial pattern in stream networks, *Front. Ecol. Environ.*, *3*(3), 138–144.

Garreta, V., P. Monestiez, and J. M. Ver Hoef (2010), Spatial modelling and prediction on river networks: Up model, down model or hybrid?, *Environmetrics*, *21*(5), 439–456.

Good, S. P., D. Noone, and G. Bowen (2015), Hydrologic connectivity constrains partitioning of global terrestrial water fluxes, *Science*, *349*(6244), 175–177.

Guthrie, R. D. (2006), New carbon dates link climatic change with human colonization and Pleistocene extinctions, *Nature*, *441*(7090), 207–209.

Hartmann, J., and N. Moosdorf (2012), The new global lithological map database GLiM: A representation of rock properties at the Earth surface, *Geochem. Geophys. Geosyst.*, *13*, Q12004, doi:10.1029/2012GC004370.

Hobson, K. A., R. Barnett-Johnson, and T. E. Cerling (2010), Using isoscapes to track animal migration, in *Isoscapes: Understanding Movement, Pattern, and Process on Earth Through Isotope Mapping*, edited by J. B. West et al., pp. 273–298 , Springer, Netherlands.

Hoppe, K. A., P. L. Koch, R. W. Carlson, and S. D. Webb (1999), Tracking mammoths and mastodons: Reconstruction of migratory behavior using strontium isotope ratios, *Geology*, *27*(5), 439–442.

Isaak, D. J., et al. (2014), Applications of spatial statistical network models to stream data, *WIREs Water*, *1*, 277–294.

Kennedy, B. P., C. L. Folt, J. D. Blum, and C. P. Chamberlain (1997), Natural isotope markers in salmon, *Nature*, *387*(6635), 766–767.

Manley, W. F., and D. S. Kaufman (2002), *Late Wisconsin Glacier Extents, Alaska PaleoGlacier Atlas version 1*, Univ. of Colo., Institute of Arctic and Alpine Research (INSTAAR). [Available at http://instaar.colorado.edu/QGISL/ak_paleoglacier_atlas.]

McGuire, K. J., C. E. Torgersen, G. E. Likens, D. C. Buso, W. H. Lowe, and S. W. Bailey (2014), Network analysis reveals multiscale controls on streamwater chemistry, *Proc. Natl. Acad. Sci. U.S.A.*, *111*(19), 7030–7035.

Peterson, E. E., and J. M. Ver Hoef (2010), A mixed-model moving-average approach to geostatistical modeling in stream networks, *Ecology*, *91*(3), 644–651.

Peterson, E. E., and J. M. Ver Hoef (2014), STARS: An ArcGIS toolset used to calculate the spatial information needed to fit spatial statistical models to stream network data, *J. Stat. Software*, *56*(2), 1–17.

Peterson, E. E., et al. (2013), Modelling dendritic ecological networks in space: An integrated network perspective, *Ecol. Lett.*, *16*(5), 707–719.

Poszwa, A., B. Ferry, E. Dambrine, B. Pollier, T. Wickman, M. Loubet, and K. Bishop (2004), Variations of bioavailable Sr concentration and Sr-87/Sr-86 ratio in boreal forest ecosystems—Role of biocycling, mineral weathering and depth of root uptake, *Biogeochemistry*, *67*(1), 1–20.

Potter, B. A., J. D. Irish, J. D. Reuther, C. Gelvin-Reymiller, and V. T. Holliday (2011), A terminal Pleistocene child cremation and residential structure from eastern Beringia, *Science*, *331*(6020), 1058–1062.

Rossi, R. E., D. J. Mulla, A. G. Journel, and E. H. Franz (1992), Geostatistical tools for modeling and interpreting ecological spatial dependence, *Ecol. Monogr.*, *62*(2), 277–314.

Ver Hoef, J. M., and E. E. Peterson (2010), A moving average approach for spatial statistical models of stream networks, *J. Am. Stat. Assoc.*, *105*(489), 6–18.

Ver Hoef, J. M., E. E. Peterson, D. Clifford, and R. Shah (2014), SSN: An R package for spatial statistical modeling on stream networks, *J. Stat. Software*, *56*(3), 1–45.

Ecological Applications, 27(2), 2017, pp. 363–377

Linking otolith microchemistry and dendritic isoscapes to map heterogeneous production of fish across river basins

Sean R. Brennan[1] and Daniel E. Schindler

School of Aquatic and Fishery Sciences, University of Washington, Seattle, Washington 98105 USA

Abstract. Production patterns of highly mobile species, such as anadromous fish, often exhibit high spatial and temporal heterogeneity across landscapes. Such variability is often asynchronous in time among habitats, which stabilizes production at aggregate scales of complexity. Reconstructing production patterns explicitly in space and time across multiple scales, however, remains difficult but is important for prioritizing habitat conservation. This is especially true for fishes inhabiting river basins due to long-range dispersal, high mortality at early life stages, complex population structure and elusive life history variation. We develop a new approach for mapping production patterns of Pacific salmon across a large river basin by integrating otolith microchemistry and dendritic isoscape models. The geographically continuous Bayesian assignment framework presented here yielded high accuracies (>90%) and relatively high precisions (precisions <4%; i.e., assignment areas of <530 river km of the 13 100 km total river length) when used to determine the natal source of known-origin juvenile Chinook salmon captured throughout the study region. Integrating these methods enabled us to base estimates of provenance and habitat use of individuals on a per location basis using strontium isotopic data throughout the continuous spatial domain of a river network. Such a framework provides substantial advantages over the more common nominal approach to employing otolith microchemistry to reconstruct movement patterns of fish. In doing so, we reconstructed the spatial production patterns of adult Chinook salmon returning to a large watershed in Bristol Bay, Alaska and illustrate the power of such an approach to conservation efforts.

Key words: Chinook salmon; habitat mosaic; habitat portfolio; isoscape; migration; otolith microchemistry; provenance; strontium isotopes.

Introduction

Conservation and habitat management are often challenged by weak understanding of how animals inhabit and move across heterogeneous landscapes over the course of their life cycles (Levin 1992). Such efforts are hampered for multiple reasons, including non-linear interactions of population dynamics and the biophysical drivers shaping habitats and population responses. This is especially true for migratory organisms (Runge et al. 2014).

Natural tracers, such as genetic and chemical signatures (e.g., trace elements, specific organic compounds, or isotope ratios) recorded in biogenic tissues, provide a powerful way to reconstruct the habitat use of highly mobile organisms (Hobson and Norris 2008). Because these tags are present in all individuals of a population, they are particularly useful for organisms that exhibit high dispersal from natal sites, high mortality at early life stages, wide ranges in life-history strategies, and extensive mixing of distinct populations during migration, foraging, or periods of human exploitation (Webster et al. 2002).

Natural tags, however, also possess important limitations requiring careful consideration. Fundamental to effectively employing natural tags is having a robust understanding of potential source populations and habitats in space and time with respect to the tracer of interest, and how the tracer may be modified during transport or biogenic incorporation (Elsdon et al. 2008, Hobson et al. 2010). Homogeneity within and among environments or populations of interest with respect to any tracer limits its utility. Natural tags are most powerful when the tag is able to distinguish populations or habitats unequivocally.

In application, the most common method for generating robust spatial baselines of natural tags involves characterizing all known source populations or usable habitats on the basis of specific tags. If significantly different, these groups or locations can then be used as the entities into which assignments of individuals of unknown origin are made. Alternatively, they can be further combined into larger groups on the basis of observed variation in the tag (those populations genetically or chemically similar) or the relevant scale for the question at hand. Such approaches are called the "nominal" method of assignment, which can be implemented in a number of ways; most often it is done using discriminant function analyses (DFA), classification trees, or their Bayesian alternatives (Wunder 2012). Although the nominal approach remains effective, it is limited by the need for users to define potential groups *a priori*, which can be arbitrary and overly rigid in many systems. This is

Manuscript received 14 June 2016; revised 22 September 2016; accepted 2 November 2016. Corresponding Editor: Michael B. Wunder.

[1]E-mail: srbrenn@uw.edu

especially true with respect to chemical signatures, which tend to be continuously distributed throughout ecosystems, such as the δ^2H and $\delta^{18}O$ signatures of precipitation across continental, latitudinal, or elevation gradients, or the $^{87}Sr/^{86}Sr$ ratios of Sr dissolved in surface waters and routed through river networks.

Recent advances in isotope-based provenance research have paved the way for a probabilistic assignment method that can be used on a per location basis throughout continuous spatial domains (Wunder 2010). In so doing, this approach allows researchers to avoid the arbitrary step of grouping geographic locations a priori and to transparently incorporate all variance-generating processes on a spatially explicit basis, e.g., as opposed to aggregating multiple locations per group in order to train a DFA model (Walther et al. 2008, Hegg et al. 2013, 2015, Brennan et al. 2015*b*). This approach is referred to as the "continuous" method of assignment. The necessary elements to apply the continuous approach for isotope-based provenance research include (1) a spatially and temporally robust characterization of isotopic variability across the geographic region of interest, called an "isoscape," and (2) a calibration, or rescaling, function relating the isotopic composition of an individual's environment at a geographic location to the biogenic tissue being analyzed for its isotopic composition. The result is a spatially explicit and continuous map of expected isotope values of an organism's tissue synthesized at a particular location. Then, by using Bayes' Rule to invert conditional probabilities, a probability density function can be computed throughout the entire spatial domain to estimate the most likely geographic origins given the isotopic information recorded in a tissue.

The continuous approach has been successfully applied to many taxa including migratory birds (Wunder and Norris 2008, Hobson et al. 2009*b*, Hobson 2011), insects (Hobson et al. 2012*a*, Flockhart et al. 2013, Vander Zanden et al. 2014), bats (Cryan et al. 2014), and recently sea turtles (Vander Zanden et al. 2015). However, it has not yet been demonstrated for migratory fishes that inhabit physically bounded, but complex, river basins. Here, we integrate three recent advances to resolve a commonly elusive and persistent problem in the ecology of migratory fish: explicitly constraining heterogeneous production throughout a vast array of potential habitat in space and time. These advances include (1) the use of strontium isotopes recorded in otoliths (Koch et al. 1992, Kennedy et al. 1997) to delineate freshwater production patterns of anadromous fish harvested during a coastal fishery (Brennan et al. 2015*b*), (2) generating river isoscapes using dendritic network models (Brennan et al. 2016), and (3) applying Bayes' Rule to map probability surfaces for natal origins of organisms based on isotopic information (Wunder 2010). By integrating these new approaches, we demonstrate how freshwater production patterns in a highly mobile fish are spatially heterogeneous and that they can be accurately mapped inter-annually at fine-spatial scales via a flexible, transparent, and powerful analytical framework.

We focus on Chinook salmon (*Oncorhynchus tshawytscha*) from the Nushagak River (Fig. 1) of western Alaska, which exhibit low genetic differentiation (Larson et al. 2014), but inhabit isotopically heterogeneous freshwater environments during their first year of life (Brennan et al. 2015*b*). Salmon populations exhibit substantial asynchrony in their production patterns (Griffiths et al. 2014), which acts to buffer their inter-annual variability in production at aggregated spatial scales. Heterogeneity in habitat, locally adapted populations (e.g., genetic population structure and life history variation), and differential responses of populations to environmental perturbations, all act to stabilize production patterns at the aggregate level (e.g., Bristol Bay-wide production vs. one of the nine major river basins flowing into the bay; Hilborn et al. 2003, Schindler et al. 2010). Because of the importance of asynchronous production of populations and habitats for stabilizing the regional production of salmon, developing ways to explicitly map such heterogeneity at multiple spatial and temporal scales simultaneously will provide unique insights into how and why production changes across space and through time. It will also help prioritize ongoing habitat conservation efforts throughout the region.

Methods

Dendritic isoscape model and data sources

We used a recently published dataset of otolith measurements (Brennan et al. 2015*b*) and a new dendritic $^{87}Sr/^{86}Sr$ river isoscape (Fig. 1; Brennan et al. 2016) to demonstrate a novel application of a Bayesian assignment framework (Wunder 2010) to map the freshwater production of Chinook salmon throughout the Nushagak River. In this system, commercial fisheries intercept Chinook salmon where the river discharges to Bristol Bay en route to natal sources distributed throughout a large river basin encompassing a vast array of diverse habitats. Brennan et al. (2015*b*) published $^{87}Sr/^{86}Sr$ ratios measured in the natal region of otoliths from adult Chinook salmon caught during a commercial fishery conducted in Nushagak Bay. We used a $^{87}Sr/^{86}Sr$ river isoscape (Brennan et al. 2016) produced using a new class of geostatistical models, spatial stream network models (SSNMs; Peterson and Ver Hoef 2010, Ver Hoef and Peterson 2010), to generate the baseline to which the natal origins of individual Chinook salmon were then assigned. $^{87}Sr/^{86}Sr$ ratios throughout this river network are temporally stable at sub- and inter-annual time scales (Brennan et al. 2015*a*). We used the best model reported by Brennan et al. (2016) as our river isoscape (Fig. 1). For the purposes of the analyses herein we considered only those streams of stream order 3 and larger because Chinook salmon are primarily associated with larger order streams. We also excluded the watershed area upstream of the Northwest Passage in the Tikchik Lakes region, because Chinook salmon are not associated with lake habitats.

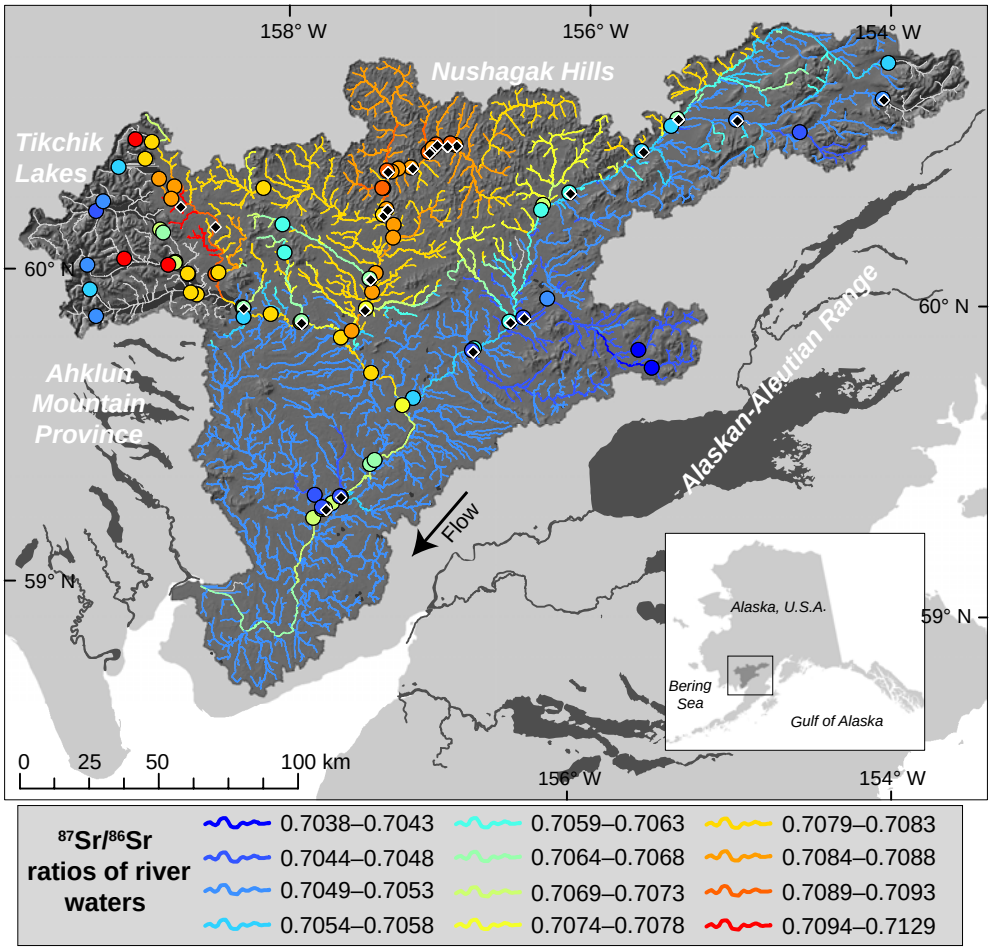

FIG. 1. The Nushagak River and variation in $^{87}Sr/^{86}Sr$ ratios in river waters (colored stream lines), redrawn from Brennan et al. (2016). Color-filled circles indicate locations of measured water ratios that were used to create river isoscape. Black-filled diamonds indicate collection sites of known-origin juvenile Chinook salmon. Colors of lines and circles use same breaks in legend. [Color figure can be viewed at wileyonlinelibrary.com]

Assigning adult fish to their natal habitat

In general, applying the continuous method of assignment to Chinook salmon intercepted during fishery harvests in Nushagak Bay, but bound for their natal origin somewhere in the Nushagak River involved (1) defining a rescaling function that relates river isoscape values to isotope values recorded in otoliths, (2) developing a model structure that incorporates the primary variance-generating processes defining the distribution of potential isotope ratios recorded in otoliths at any location within the river network, and (3) applying Bayes' Rule to conditional probabilities of isotope ratios at all locations (constructed from steps 1 and 2) to generate probability density functions across the river basin.

Because of the clearly defined relationship between ambient water and otolith $^{87}Sr/^{86}Sr$ ratios (Barnett-Johnson et al. 2008, Muhlfeld et al. 2012, Brennan et al. 2015*a, b*), we assumed a rescaling function where the $^{87}Sr/^{86}Sr$ ratio of an otolith, o_i, synthesized at location j is equivalent to the $^{87}Sr/^{86}Sr$ ratio of the river water flowing past location j, r_j, according to:

$$o_{i,j} = r_j + \varepsilon \quad (1)$$

where r_j is the predicted isotope ratio at location j from the dendritic river isoscape model of (Brennan et al. 2016) and ε is the normally distributed error term associated with all processes that relate the river water isotope ratio at location j to an otolith's isotope ratio synthesized at location j.

Next, we constructed a variance model that included three primary sources of variance for otolith $^{87}Sr/^{86}Sr$ ratios synthesized at any location within the network: analytical error, within-population variance, and the error associated with isoscape estimates at each location throughout the network (Appendix S1: Fig. S1). We assumed all three errors were normally distributed and combined them via

$$\sigma_{\text{combined}} = \sqrt{\sigma^2_{\text{analytical}} + \sigma^2_{\text{within}-pop} + \sigma^2_{\text{isoscape}}} \quad (2)$$

where $\sigma^2_{\text{analytical}}$ is the variance of repeat measurements of an internal marine shell standard (Brennan et al. 2015*b*). $\sigma^2_{\text{within}-pop}$ reflects the variance of otolith ratios among individuals captured at the same known-origin site. This was estimated by subtracting $\sigma^2_{\text{analytical}}$ from the prediction intervals of a water–otolith regression of juvenile Chinook salmon (n = 146; 5–10 individuals per site) collected from throughout the Nushagak basin (Brennan et al. 2015*b*). Regression prediction intervals reflect both analytical and within population variance. Last, $\sigma^2_{\text{isoscape}}$ represents the error associated with the isoscape model's estimation at any location (Brennan et al. 2016), which is the squared standard error of each prediction (Garreta et al. 2010). The residuals of this river isoscape model approximated normality (Appendix S1: Fig. S2). The former two errors were defined as single values ($\sigma^2_{\text{within}-pop} = 1.1 \times 10^{-4}$; $\sigma^2_{\text{analytical}} = 5.5 \times 10^{-5}$) applied at all locations throughout the network, while the latter represents a raster surface of errors computed along the network from Brennan et al. (2016). Thus, the general form of the probability density function for any o_i is

$$o_j | r_j \sim N(r_j, \sigma^2_{\text{combined}}). \quad (3)$$

This equation defines the probability distribution of $^{87}Sr/^{86}Sr$ ratios synthesized into otoliths at location j within the network given the isoscape ratio of river water at j taking into account the primary variance-generating processes. However, from a provenance research perspective, we are more interested in the inverse of this statement, i.e., the probability that location j is the true origin given an otolith's isotope ratio. As such, we used Bayes' Rule to invert the conditional probabilities from above. The algorithm we used to apply Bayes' Rule is explained in detail in Wunder (2010) and is similar to Vander Zanden et al. (2015). Briefly, here, Bayes' Rule was written as

$$P(J=j|O=o_{i,j},R=r_j)=\frac{P(O=o_{i,j}|R=r_j)P(J=j)}{\int P(O=o_{i,j}|R=r_\xi)P(J=\xi)d\xi} \quad (4)$$

where J is a random variable defining the posterior probability distribution for all locations j within a river network composed of ξ locations, $P(O = o_{i,j}|R = r_j)$ is the conditional probability distribution for otolith $^{87}Sr/^{86}Sr$ ratios from Eq. 3, and $(P(J = j))$ is the probability the j is the location in the absence of isotope information (i.e., the prior probability). This computes the probability that location j is the true origin given the isotope ratio measured in an otolith and the ratios existing throughout the river network. The denominator integrates to a constant and so the probability density function is proportional to the numerator

$$P(J=j|o,r_j)\propto\left\{\frac{1}{\sqrt{2\pi\sigma^2_{\text{combined}}}}e^{-\frac{(o-r_j)^2}{2\sigma^2_{\text{combined}}}}\right\}I_{\text{habitat}} \quad (5)$$

where j is a location within the river network, o is the $^{87}Sr/^{86}Sr$ ratio measured in the otolith of a fish of unknown origin, and I_{habitat} is a prior on location, such that only the areas within the river known to support Chinook salmon populations were considered (i.e., a multiplier of zero was assigned to locations in the network that are not known to produce Chinook salmon, such as the Tikchik Lakes region; Fig. 1).

During our comparison of different approaches to summarize assignments across the population of returning Chinook salmon (see *Estimating basin-wide production patterns*), we also used an index of habitat suitability for spawning Chinook salmon in the Nushagak River (Woll et al. 2014) as a prior, $P(J = j)$ in Eq. 4 and I_{habitat} in Eq. 5 (Appendix S1: Fig. S3). Once posterior probabilities were computed across the network, they were normalized so that the probabilities of all locations summed to 1. To aid in visualization and to compare among all individuals, these were then rescaled so that values ranged from 0 to 1 by dividing by the maximum posterior probability (Fig. 2).

Model accuracy and precision

To assess the accuracy of the model to correctly assign fish back to the correct source location, we used juvenile Chinook salmon (n = 146) captured at specific locations throughout the watershed (Brennan et al. 2015*b*). These individuals were not used to build the isoscape; as such, they provide an independent test of model accuracy and precision. We defined the accuracy as the proportion (presented as a percentage) of correctly assigned individuals to known locations. The assignment of each individual corresponds to those reaches of river with posterior probabilities above a user-defined probability threshold. Each fish's assignment is transformed into a binary surface indicating those locations most likely and those locations least likely at the defined probability threshold. If the known location of a fish is included in the set of most likely locations, then that fish was considered as correctly assigned. To demonstrate how the accuracy changes as the probability threshold becomes more constrained (i.e., closer to 1), we computed the accuracy over a range of thresholds (0–0.99) as in (Vander Zanden et al. 2014).

We estimated model precision as the proportion of the river network where a positive assignment could be made; high precision corresponds to low proportions and vice versa. The amount of suitable salmon habitat (as kilometers of river) corresponding to an individual's assignment was computed at a specified posterior probability threshold (ranging from 0 to 0.99) and compared to the total amount of habitat of the Nushagak River (i.e., a proportion of km/km of the total habitat in the system, 13100 km, which is the total length of all third-order and higher streams). To demonstrate how assignment precision changed as a function of the probability threshold, we computed the mean and standard deviation of assignment precisions of all known-origin fish over the

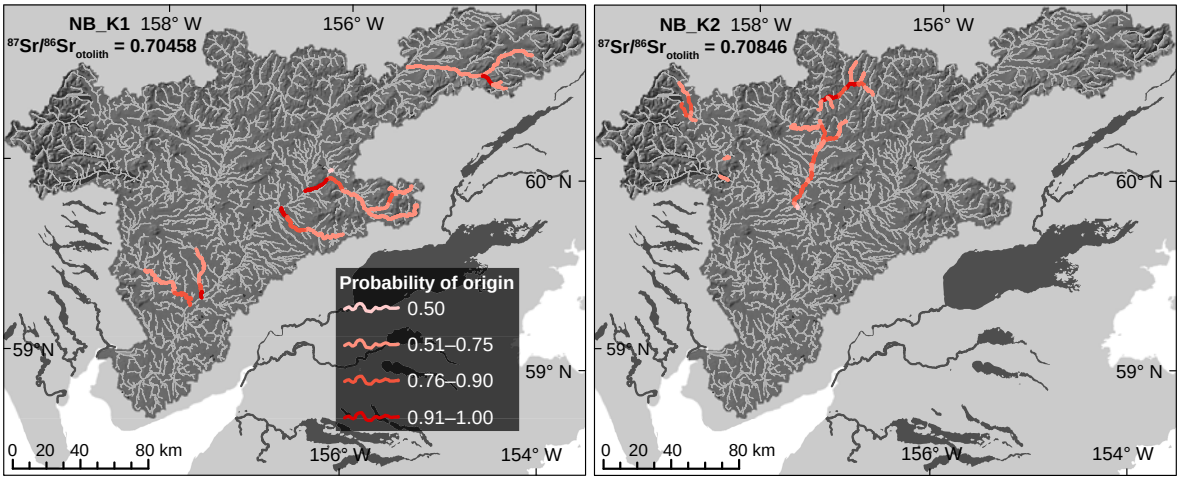

FIG. 2. Examples of the posterior probability surfaces of individual Chinook salmon (NB_K1 and NB_K2) with $^{87}Sr/^{86}Sr$ ratios of 0.70458 and 0.70846. Only those locations with probabilities >0.50 are colored red, all others are gray. [Color figure can be viewed at wileyonlinelibrary.com]

range of probability thresholds. Additionally, we tested whether the precision of assignments varied as a function of a fish's otolith isotope ratio by computing how the precision changed over the range of observed otolith isotope ratios in known-origin fish. This test is essentially an accounting of the relative abundance of predicted isotope values throughout the Nushagak River (some ratios are more spatially restricted than others).

To further assess model accuracy and precision, we also used odds ratios (the odds of being correct vs. incorrect) to evaluate the performance of the isotope-based model to correctly assign known-origin juvenile Chinook salmon compared to what would be expected by chance alone (Wunder 2012). We used the same procedure as above to determine "likely" and "unlikely" regions, but evaluated the accuracy and precision over a range of expected odds ratios (0.01:1 to 99:1). Here, each location in the probability surface of each individual was normalized by its sum and the locations corresponding to the highest probabilities above a set proportion of the sum were designated as "likely" (i.e., the odds of being correct) and all other locations were determined as "unlikely" (i.e., the odds of being incorrect). For example, for an odds ratio of 2:1, the "likely" locations would constitute the top 67% of all probabilities, whereas the "unlikely" locations would correspond to the lowest 33%. Thus, we would expect 2:1 odds of determining the correct location; correctly assigning >67% of known-origin fish would indicate the isotope-based model is more accurate than expected.

Estimating basin-wide production patterns

To estimate the overall production patterns across the Nushagak River basin in 2011, we compared three different approaches to summarizing the assignments made for all Chinook salmon: (1) a "binary transformation" approach (Hobson et al. 2009*b*, Flockhart et al. 2013, Vander Zanden et al. 2015), (2) an approach that simply sums the probability surfaces of all individuals, referred to as the "summed probability" approach hereafter, and (3) an approach that uses a non-uniform prior of habitat suitability for Chinook salmon (referred to as the "habitat prior" method hereafter). The former two approaches use a uniform prior across all potential stream habitats. We compared these three approaches by splitting the entire basin into its major sub-basins (n = 29) and computing each sub-basin's proportion of the basin-wide production. Additionally, we also compared these sub-basin estimates to the Strontium Isotopic Groups (SIGs) of Brennan et al. (2015*b*), which were determined therein by grouping streams *a priori* based on isotopic and geographic similarities (Table 1).

To assign adult Chinook salmon back to their natal sources using the binary transformation approach, we defined a relative probability threshold that designated locations as "likely" and "unlikely," such that all likely locations were considered to be the assignment area. To date, this has been the most common way to summarize patterns at the population level using a continuous approach (Hobson et al. 2009*a*, 2012*a*, Flockhart et al. 2013, Vander Zanden et al. 2015). The threshold was determined by evaluating the precision and accuracy over a range of relative probability thresholds and selecting the threshold that provided the best trade-off between accuracy and precision. Once determined, those locations that corresponded to relative posterior probabilities greater than the set threshold were determined to be the assignment area for each fish from the 2011 sample (n = 255). The result was 255 binary rasters of the same extent and resolution, where all locations with a value of 1 delineated the assignment for each fish. These rasters were then summed, such that the value in each grid cell corresponded to the number of fish assigned to that

TABLE 1. Comparison of production estimates between a nominal approach (Strontium Isotopic Groups [SIGs] of Brennan et al. [2015*b*]), and the three continuous approaches considered here, the binary transformation, summed probability, and habitat as prior methods.

	Production estimates			
	Nominal	Continuous		
SIG	SIG	Binary transformation	Summed probabilities	Habitat as prior
SIG1	0.22	0.25	0.23	0.25
SIG2	0.22	0.18	0.18	0.19
SIG3	0.10	0.10	0.07	0.09
SIG4	0.04	0.03	0.02	0.02
SIG5	0.11	0.06	0.04	0.04
SIG6	0.27	0.34	0.22	0.25
SIG7	0.05	0.03	0.04	0.05

Notes: SIGs were determined by considering isotopic and geographic similarities (see Brennan et al. 2015*b*). The small, low-gradient tributaries to the lower river were not included in these comparisons, as they were not considered by Brennan et al. (2015*b*).

location using the defined threshold. In the second approach, we did not apply a binary transformation to the probability surface to any of the individuals. Instead, the probability surfaces of all individuals were simply summed. The third approach, applied a non-uniform prior describing variation in habitat suitability for spawning Chinook salmon across the Nushagak River (Woll et al. 2014; i.e., via Eq. 5). The resulting probability surfaces of all individuals were then simply summed, as in the second approach. This prior employed a habitat suitability index that ranked Chinook spawning habitat on a five-point integer scale (0, not suitable, to 4, highly suitable), which was determined on the basis of well-known geomorphological features of streams preferred by spawning Chinook salmon (e.g., channel width and depth; Woll et al. 2014). By using this index, we assumed that in the absence of isotope information the probability that a Chinook salmon was produced from any particular stream reach is proportional to its habitat suitability ranking (e.g., a stream reach with a rank of 4 is four times as likely as a stream reach with a rank of 1, and so on).

In all three approaches, we normalized the sum of all assignments (i.e., binary transformation approach) or the sum of all probabilities (i.e., summed probability approaches) at each location by the basin-wide sum of each respective metric. The production estimates for the entire basin for each method summed to 1. We then estimated the proportion of the 2011 run that was produced from the different major sub-basins within the watershed in order to compare how the approaches differed.

RESULTS

Accuracy and precision of known-origin juveniles

The model was >90% accurate for all relative probability thresholds <0.75 when determining the natal locations of known-origin juvenile Chinook salmon; the accuracy decreased rapidly as thresholds became more restrictive toward 1 (Fig. 3a). Precision of assignments was poor at low thresholds (<0.45), at which point the precision improved substantially to <4% of the total river length for thresholds >0.50 (Fig. 3b). Thus, we used a relative posterior probability threshold of 0.50 (i.e., relative posterior probabilities >0.50) to generate the production heat-maps for the 2011 fishery harvest when employing the binary transformation method. At this threshold, the accuracy was 96% and the precision was 340 ± 72 km. Precision of assignments also changed as a function of the isotope ratio in an otolith, where ratios between 0.7071–0.7073 yielded the most precise estimates (Fig. 3c) because these mapped on to habitat locations with more spatially restricted isotope values. Using odds ratios of >0.12:1 (i.e., expected accuracies of >0.11; Appendix S1: Fig. S4) the model yielded >90% correct determination of the known-origin locations of juvenile Chinook salmon. Precision of assignments for these odds ratios (>0.12:1) were <3% of the total river length.

Assignment of harvested adults to natal habitat

Using the three assignment approaches outlined here we determined that the relative production of Chinook salmon caught in 2011 was spatially heterogeneous across the Nushagak River basin, where the largest areas of production were in the Upper Nushagak River, the Mulchatna River, and its tributaries draining the Alaskan-Aleutian Range (AAR; Fig. 4). Overall, these results generally agreed with our previous estimates of production using a nominal approach (Table 1; Brennan et al. 2015*b*). The two dominant age-classes returning to the Nushagak in 2011 (age 1.3 and 1.4, i.e., fish that spent 1 yr as a juvenile in freshwater and 3 and 4 yr, respectively, in the ocean) exhibited similar production patterns (Fig. 5), where the Upper Nushagak River was the most productive section of the river. The distribution of age 1.5 individuals was more evenly spread across the basin, but with regions of relatively high production from the AAR tributaries along the eastern side of the river basin (Fig. 5).

The binary transformation, summed probability, and non-uniform prior of habitat suitability methods

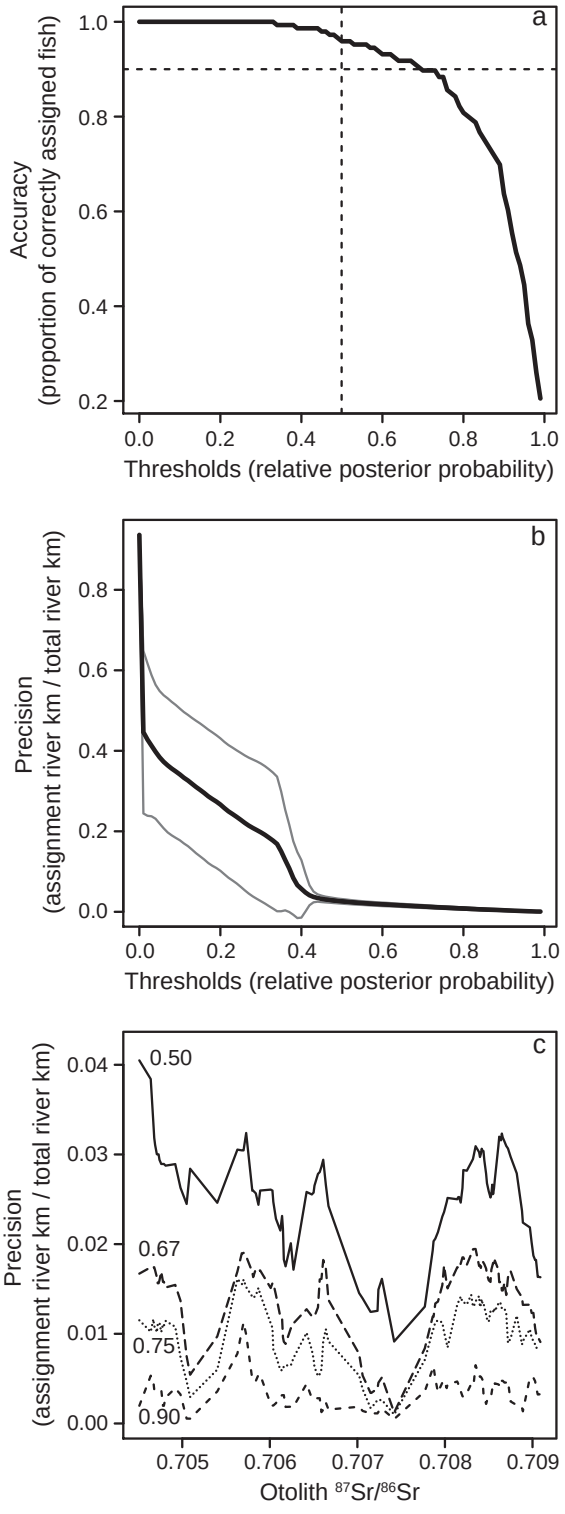

FIG. 3. (a) Accuracy and (b) precision of assignments made using Bayesian assignment approach outlined herein computed using individual juvenile Chinook salmon (n = 146) of known origin. (c) How the isotope ratio of fish otoliths influence the precision of assignments over thresholds of 0.50, 0.67, 0.75, and 0.90 (numbers on plot), i.e., accounting for the relative abundance of predicted isotope ratios throughout river basin. Dotted lines in panel a correspond to relative posterior probability threshold used during binary transformation. Thin lines in panel b correspond to standard deviation of precision estimates.

generated similar production patterns when comparing estimates for the major sub-basins within the watershed (Table 2). All three identified the Upper Nushagak River, Mulchatna River, and AAR tributaries as the principal producers of Chinook salmon. However, the binary transformation approach assigned zero fish to regions of the river characterized by high uncertainties in the $^{87}Sr/^{86}Sr$ isoscape (Brennan et al. 2016). These regions were consistently those where the water isotope ratios were estimated via extrapolation in the isoscape model (Brennan et al. 2016). As a result, the probabilities of these reaches were always <0.5, and were determined as "unlikely" during binary transformation. In contrast, both summed probability approaches assigned some proportion of fish to these regions because the probabilities of these stream reaches were non-zero for individual fish. The production estimates of these regions, however, were markedly less (i.e., <50%) when compared to isotopically similar reaches characterized by smaller errors. The estimates made via all three methods scaled positively with basin size (Table 2 and Appendix S1: Fig. S5). Production estimates made via the summed probability approach exhibited the strongest positive correlation with basin size (r > 0.9, Appendix S1: Fig. S5). As a result, the larger basins were estimated to have produced larger proportions of the 2011 run. When compared to the estimates based solely on the amount of suitable habitat, sub-basins differed by 0.2–41.5% when including isotopic information using Bayes' Rule (Table 2). This illustrates that some sub-basins produced more or less fish than what is expected based on the amount of suitable habitat alone.

DISCUSSION

By integrating river isoscapes built using dendritic network models, a geographically continuous Bayesian assignment framework, and otolith microchemistry, we reconstructed the production patterns of Chinook salmon across a large river basin with high precision and accuracy.

Model performance

There was a trade-off between precision and accuracy across a range of posterior probability thresholds (Fig. 3). The accuracy decreased (i.e., the probability of an incorrect assignment increased) as the threshold became more restricted toward 1; the precision of assignments increased (i.e., fish were assigned to increasingly smaller proportions of the river basin) as the threshold became more restrictive toward 1. Both of these relationships reflect the fact that, by successively constraining the threshold toward 1, the size of the geographical area

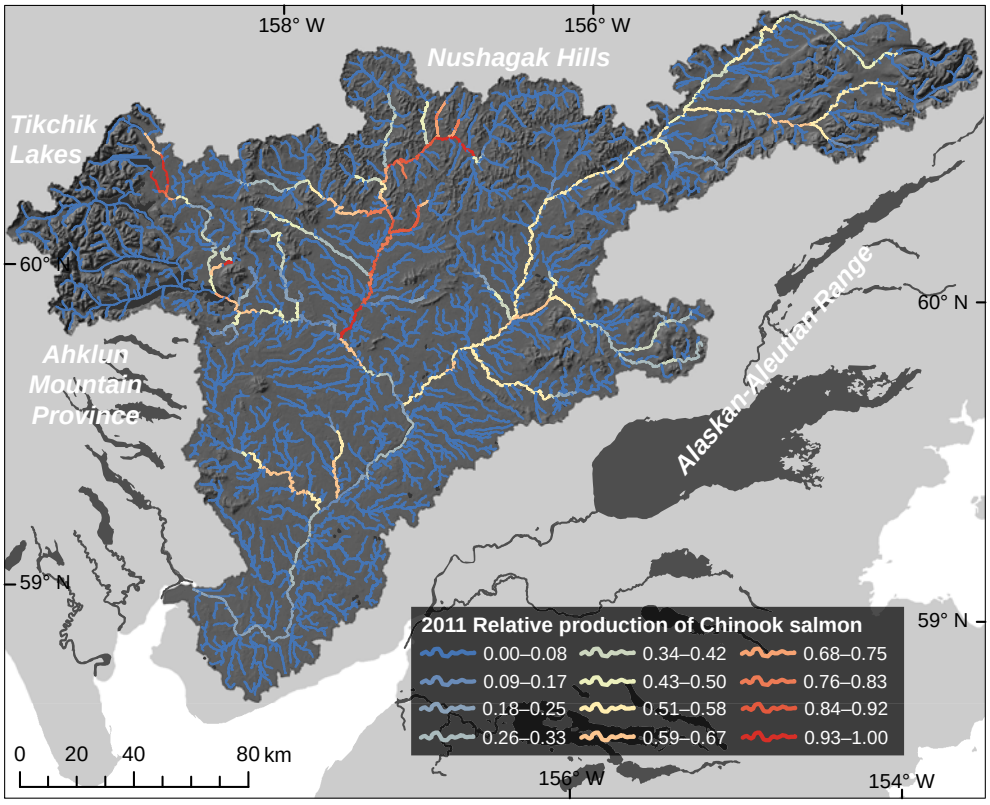

FIG. 4. Heat-map of the relative production of Chinook salmon returning to the Nushagak River in 2011. To ease visualization, only those stream reaches with relative posterior probabilities >0.5 for each individual were considered as the region of its origin (see *Estimating basin-wide production patterns*). We scaled the production estimates at each location by the maximum proportion of production (3.74×10^{-5}) computed throughout the basin; as such values range from 0 to 1. [Color figure can be viewed at wileyonlinelibrary.com]

corresponding to each assignment decreases. An assignment with a smaller geographical area will have a greater tendency to misclassify an individual relative to its true source location. Thus, by constraining the geographical area, the precision of assignment to natal habitat increases but the likelihood of a misclassification increases. By testing our assignment model with an independent validation set of known-origin juvenile Chinook salmon captured throughout the river network, the model still yielded high accuracies (>90% correct classifications) with relatively high precisions (<0.04 of all available habitat, or <530 river km of the 13100 km available). Although some river water isotope ratios are more common than others (i.e., 0.7073–0.7075), the precision is relatively constrained at all isotope ratios (Fig. 3c). Furthermore, over the entire range of odds ratios evaluated (Appendix S1: Fig. S4) the assignment model demonstrated substantial improvements in both accuracy and precision relative to what would be expected at any defined odds ratio (Appendix S1: Fig. S4). Because accuracies of 90% often represent the lower limit for applying assignment models in Alaskan salmon management (Dann et al. 2013), the isotope-based assignment model here is amenable to such applications. Evaluating the model over a range of user-defined relative probability thresholds and odds ratios enabled the determination of the thresholds at which the model performed well enough to satisfy such a guideline.

Advantages of building variance models from first principles

One of the advantages of the geographically continuous approach to assignment is being able to identify which variance-generating processes have the greatest effect on assignment efficacy. There are multiple ways to estimate $\sigma^2_{\text{combined}}$ and this remains an important topic of research, but one of the most useful ways is to partition the variance and build it from first principles (Wunder 2010, Bowen et al. 2014). Here, the error in our isoscape strongly influenced the locations of assignments. Specifically, the highest posterior probabilities of assignments were biased toward areas where the isoscape predictions have low error. Because areas of low error are near to where $^{87}Sr/^{86}Sr$ water measurements were made and where $^{87}Sr/^{86}Sr$ ratios were estimated via interpolation along the network, assignments are biased toward regions proximal to observations and those areas

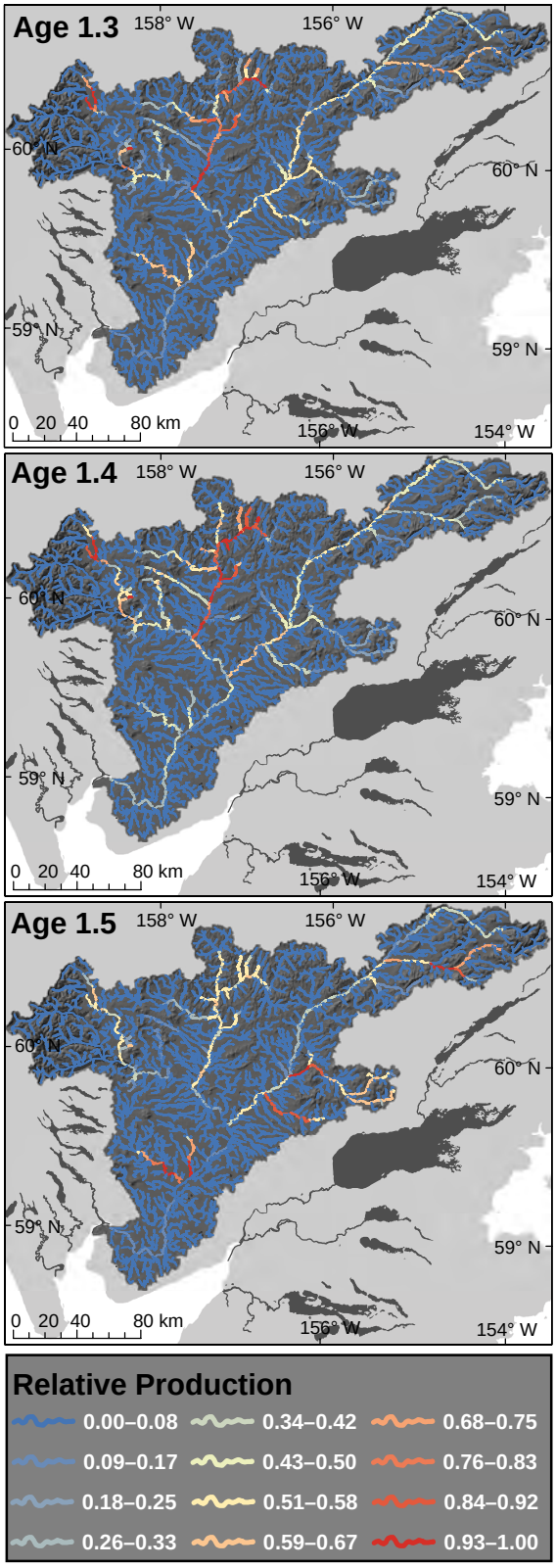

FIG. 5. Age-specific relative production heat maps of Chinook salmon returning in 2011 including age 1.3, 1.4, and 1.5 (the first number indicates the number of years spent in freshwater; the second number indicates the number of years spent in the ocean before returning to spawn) determined via binary transformation. To ease visualization, we scaled the age-specific production estimates at each location by their maximum proportion of production computed throughout the basin; as such values range from 0 to 1 (maximum proportion of age 1.3 = 3.98×10^{-5}, age 1.4 = 3.85×10^{-5}, and age 1.5 = 4.11×10^{-5}). [Color figure can be viewed at wileyonlinelibrary.com]

situated downstream along the network. The distribution of posterior probabilities depends on both the difference between the otolith and river water ratios, and the combined error at each location (i.e., Eq. 5). Thus, those locations with larger errors have relatively lower posterior probabilities. For example, if the difference between an otolith's isotope ratio and the river water was the same at two different locations, but the error of one location was 0.0002 (e.g., estimated via interpolation), and the error of the other location was 0.0007 (e.g., estimated via extrapolation upstream): the former location would have a posterior probability three times the latter, as computed by Eq. 5. The overall result is that very few fish were assigned to regions where the isoscape prediction errors ($\sigma_{isoscape}$) those areas estimated via extrapolation in the isoscape model. were >0.0006 in the $^{87}Sr/^{86}Sr$ ratio, i.e., Because the river isoscape includes only 3rd order and larger streams (Brennan et al. 2016), it is likely that some Chinook salmon are produced, or at least rear, in some of the reaches characterized by errors >0.0006. Thus, the regions of the Sr isoscape where $^{87}Sr/^{86}Sr$ ratios were estimated via extrapolation may understate the actual production from those reaches. Although this is an obvious limitation, the current $^{87}Sr/^{86}Sr$ sampling distribution of the Nushagak does include the large majority of the tributaries known to produce Chinook salmon.

Explicitly incorporating each source of variance associated with assigning individuals to their natal locations enables the identification of which sources of variance would benefit most from additional research effort. Because of the conservative nature of $^{87}Sr/^{86}Sr$ ratios, both analytical and within-population variances are relatively well constrained herein and are likely not to improve much with additional effort. However, given the biases driven by the range of errors in the isoscape, additional sampling would substantially improve the model at specific locations known to support Chinook salmon (e.g., above "Big Bend" in the Upper Nushagak, upper Mosquito, and Iowithla Rivers). That said, the model herein realistically reflects our abilities to determine provenance and habitat use throughout a continuous spatial domain using isotopic information recorded in otoliths.

TABLE 2. Production estimates for the individual sub-basins within the Nushagak River using different summarization methods via a geographically continuous assignment framework: binary transformation, summed probability, and habitat as prior methods.

Sub-basin	Prop. of total stream length	Production estimates (proportion of total)					No. Chinook salmon in 2011 returning to Nushagak sub-basins in 2011 run				
		Binary	Summed prob.	Habitat as prior†	Habitat only‡	Comparing prod. estimates§	Binary	Summed prob.	Habitat as prior	Habitat only	Corresp. SIG
Arrow	0.011	0.023	0.010	0.011	0.014	−17.6	2518	1053	1229	1492	SIG3
Chichitnok	0.022	0.013	0.026	0.032	0.029	10.4	1407	2807	3429	3107	SIG7
Chilchitna	0.021	0.020	0.024	0.025	0.023	7.9	2169	2555	2729	2529	SIG2
Chilikadrotna	0.046	0.067	0.043	0.054	0.052	4.6	7273	4660	5883	5622	SIG1
Fifteenmile	0.004	0.013	0.005	0.005	0.005	15.9	1355	557	582	502	SIG7
Harris	0.010	0.005	0.008	0.009	0.013	−31.1	569	860	996	1445	SIG4
Iowithla	0.017	0.000	0.018	0.020	0.020	−1.3	0	1975	2149	2179	SIG1
KingSalmon	0.038	0.049	0.044	0.053	0.050	6.8	5292	4788	5773	5407	SIG6
Klutapuk	0.005	0.007	0.007	0.009	0.008	13.1	757	708	926	818	SIG7
Klutuk	0.016	0.028	0.017	0.020	0.019	4.2	3032	1883	2120	2035	SIG1
Klutuspak	0.008	0.023	0.007	0.012	0.014	−19.6	2462	799	1245	1549	SIG3
Koktuli	0.053	0.075	0.054	0.061	0.067	−7.9	8142	5785	6625	7189	SIG1
Kokwok	0.062	0.041	0.068	0.066	0.066	1.2	4467	7373	7163	7076	SIG1
LittleKingSalmon	0.005	0.005	0.005	0.006	0.007	−9.9	511	489	641	711	SIG3
Small tribs. to Lower River mainstem	0.139	0.001	0.150	0.083	0.085	−2.0	115	16229	8959	9143	N/A¶
Small tribs to Middle River mainstem	0.042	0.000	0.045	0.034	0.034	−0.6	27	4888	3679	3700	N/A¶
Lower Nushagak main stem only	0.023	0.043	0.018	0.016	0.026	−38.1	4608	1954	1750	2829	SIG4/SIG3
Middle Nushagak main stem only	0.006	0.019	0.007	0.008	0.007	5.6	2019	784	828	784	SIG5
Mosquito	0.019	0.003	0.015	0.020	0.028	−28.0	312	1649	2169	3013	SIG3
Mulchatna mainstem	0.109	0.114	0.118	0.117	0.117	0.2	12345	12710	12681	12652	SIG2
Nuyukak	0.029	0.034	0.032	0.031	0.030	3.2	3713	3486	3393	3287	SIG5
Oldman	0.014	0.017	0.012	0.016	0.020	−22.6	1806	1293	1697	2191	SIG2
Polly	0.003	0.016	0.004	0.005	0.003	41.5	1705	444	529	374	SIG6
Stuyahok	0.025	0.040	0.027	0.032	0.033	−2.5	4270	2877	3493	3583	SIG1
TikchikLakes	0.066	0.008	0.003	0.001	0.001	1.1	843	275	72	71	#
Tikchik	0.040	0.076	0.029	0.039	0.043	−9.6	8214	3185	4236	4688	SIG6
UpperMultch	0.059	0.068	0.062	0.065	0.064	0.7	7303	6644	6985	6939	SIG2/SIG3
UpperNushagak mainstem	0.102	0.160	0.129	0.131	0.108	21.2	17254	13960	14175	11699	SIG6
Vukpalik	0.008	0.032	0.012	0.017	0.013	34.7	3481	1313	1847	1371	SIG6

Notes: Total run in 2011 of Chinook salmon to the Nushagak River was 107989 (Jones et al. 2011). Prop., proportion; prob., probability; corresp., corresponding.

† Including habitat suitability as non-uniform prior on isotopes.

‡ Only considering spawning habitat suitability.

§ Using isotope model vs. expected based on amount of suitable habitat (% difference of former to latter).

¶ Not considered by Brennan et al. (2015*b*) in SIG determinations.

See prior, this region is not Chinook salmon habitat.

The continuous vs. nominal approach for otolith microchemistry

Although the continuous approach to assignment has broad implications for reconstructing the provenance and movements of fish using otolith microchemistry, this study represents its first demonstration. Currently, the nominal method has been the only approach used for determining provenance and habitat-use of fish using otolith microchemistry. Most notably, DFAs are the most common (Mercier et al. 2011). Although these remain effective approaches in many settings, they can be arbitrary in their construction and also overly constrained due to the necessity of a priori grouping procedures. This is especially important given the continuous nature by which chemical and isotopic tracers are distributed throughout aquatic ecosystems. By adopting a Bayesian framework, the distribution of tracer data also need not be normal and other distributions can be used (Wunder 2010).

In contrast to the nominal method, a continuous approach that is based on a realistic baseline of the spatially continuous distribution of isotope variation, allows each location in a network to be assessed relative to all other locations as a function of isotope information. Although, we only present this method for $^{87}Sr/^{86}Sr$ ratios in otoliths, this framework can also be multivariate (e.g., Vander Zanden et al. 2015) or used similarly with other singular tracers (e.g., element-to-calcium ratios, δ^2H, and $\delta^{18}O$ values). To do so, however, still requires constraining the fundamental features and assumptions of provenance studies including a characterization of each tracer in space and time, and a well-defined rescaling function describing how the tracer routes from the environment into the otolith. Constraining a rescaling function is likely the most important step in a continuous assignment framework, especially when applying tracers that are modified during biogenic incorporation via physiological, environmental, ontogenetic, or species-specific effects (Walther et al. 2010, Sturrock et al. 2015).

A primary advantage of using $^{87}Sr/^{86}Sr$ within this framework is the fact that the ratios recorded in otoliths directly reflect those of the habitats of fish in a 1:1 fashion. This feature alone substantially simplifies interpretation of $^{87}Sr/^{86}Sr$ ratios in otoliths relative to other tracers or tissues. For example, constraining a rescaling function has been one of the most challenging aspects and sources of uncertainty in the δ^2H system (the isotope system most commonly used) when rescaling δ^2H of precipitation isoscapes to the δ^2H of keratinous materials of organisms (Wunder 2010, Hobson et al. 2012*b*, Bowen et al. 2014, van Dijk et al. 2014, Vander Zanden et al. 2014). Mischaracterizations of rescaling functions may also lead to erroneous results (Wittenberg et al. 2013). Similarly, because many tracers in fish otoliths are also subject to similar sources of uncertainty, such as physiological, environmental, temporal, ontogenetic and species-specific effects on elemental incorporation into otoliths (Campana 1999, Walther et al. 2010, Sturrock et al. 2015), careful attention will be required when using other otolith tracers within a continuous framework. However, the clearly defined relationship between ambient water and otolith $^{87}Sr/^{86}Sr$ ratios makes Sr isotopes particularly well suited for applying the continuous approach to migratory fish.

Characterizing production patterns via binary transformation and summed probability methods

Overall, the relative production patterns estimated by the binary, summed probability, and non-uniform prior on habitat methods were similar (Table 2), but their differences highlighted important implications for applying the continuous method to migratory fish. In particular, the binary method concentrated assignments (and therefore the proportion of returning fish) into reaches characterized by low uncertainty in the isoscape model (Eq. 2). The summed probability methods did as well, but less so. The result was that the summed probability methods tended to spread the proportion of fish out among stream reaches more than the binary method. To illustrate this point, Fig. 6 shows how the production patterns within the King Salmon sub-basin varied at these finer spatial scales depending on the summarization method employed (Fig. 6). This difference was driven primarily by the fact that, when the summed probability method was used, those reaches with probabilities less than a set threshold still received some non-zero proportion of the production. Thus, how the uncertainty in our isoscape varied in space influenced the relative production patterns within any given sub-basin. When comparing production patterns among methods at the sub-basin level, however, the estimates were more similar (Table 2 and Fig. 6). Such results highlight the fact that useful information may be lost when applying a binary threshold to probability surfaces of individuals. This is especially true if an individual's probability surface is substantially influenced by the spatially explicit error structure of the underlying isoscape with which assignments are determined.

Both the binary and summed probability methods produced spatial distributions of Chinook salmon production that scaled strongly with the proportion of stream length within each sub-basin ($r > 0.57$), but the relationship was more pronounced in the latter approaches (Appendix S1: Fig. S5). Because the proportion of each sub-basin was estimated by summing the proportion of all reaches within that basin, the larger basins accrued larger proportions. This also led to differences between sub-basins, which are isotopically similar (e.g., Koktuli and Stuyahok Rivers), but differing in their proportion of the river basins total stream length. Furthermore, by not applying a binary transformation when employing a summed probability method, there were more reaches with non-zero values contributing to each sub-basin's sum, leading to its stronger relationship with stream

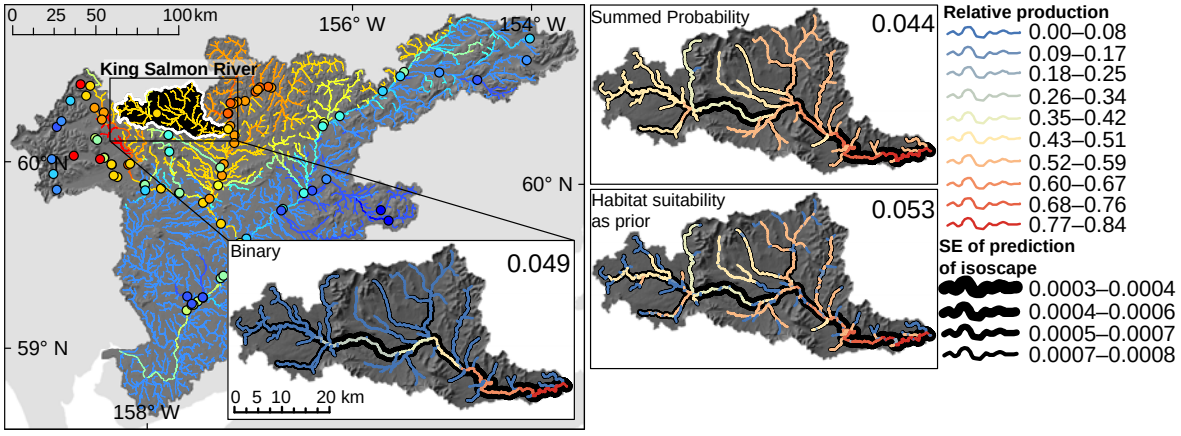

FIG. 6. Example comparison of relative production estimates within a sub-basin (King Salmon River) using methods of binary transformation, summed probability, and habitat suitability as a prior. Each basin-wide relative production estimate is indicated in the upper-right corner (from Table 2). The relative production estimates within each basin (colored lines) of each method have been scaled by the maximum proportion of production computed by each respective method, so that values scaled from 0 to 1 (note that the maximum value was not within the King Salmon River). The heavy black streamlines have been scaled inversely proportional to the standard error of predictions of the river water isoscape. [Color figure can be viewed at wileyonlinelibrary.com]

length. This relationship also drove the large difference between methods in production estimates of the small low gradient tributaries flowing into the mainstem of the lower Nushagak River (Table 2). Probabilities were never >0.5 in these stream reaches, as such their relative production as estimated via the binary transformation method, was near zero. However, by not applying a threshold, the summed probability method estimated a much larger proportion even though the maximum probabilities for any individual were always <0.5. The streams in this part of the river are very low gradient and sinuous, features that naturally increase stream length, but they are also not suitable for spawning Chinook salmon. The habitat data available for this lower river region (Woll et al. 2014) indicate that the majority of stream reaches within these tributaries have low suitability for spawning Chinook salmon (>88% of stream reaches are not suitable or have low suitability). As such, by treating all stream reaches as equally suitable during the summed probability assignment method (i.e., uniform prior across all streams of third-order or higher), the relative production was likely overestimated in the low gradient tributaries.

When we incorporated habitat suitability as a prior into our assignment algorithm, the summed probability production estimates changed substantially for the regions where large proportions of the stream reaches within a sub-basin were mapped to be of low suitability for spawning Chinook salmon. In particular, the production estimate for the small tributaries flowing into the main-stem of the lower Nushagak River decreased by half (Table 2). Overall, these differences highlight the advantages of coupling this Bayesian assignment approach with habitat suitability estimates in the form of informative priors describing habitat features. Similarly, the relative abundance of respective populations has been shown to be important for isotope-based Bayesian assignment frameworks (Royle and Rubenstein 2004). Such an approach, however, requires reliable estimates of relative abundance and an assumption that abundance patterns are fixed in time. Because individual salmon populations exhibit asynchronous production patterns (Schindler et al. 2010), the relative abundances of different populations distributed across a variety of habitats likely vary temporally at multiple spatial scales. Since abundance patterns of different populations within the Nushagak are not known, and since such patterns likely exhibit asynchronous temporal variability, we used instead a prior informed by known geomorphic features of rivers that are preferred by Chinook salmon. Geomorphic habitat features (e.g., channel width or depth) are also generally more stable with respect to time and covary strongly with species-specific habitat preferences of salmonids (Whited et al. 2012, 2013). Thus, such geomorphic attributes of streams are effective as priors within a spatially continuous Bayesian assignment framework for migratory fish. Ultimately, coupling the isotope-based continuous method of assignment with habitat models, which assume that suitable aquatic habitat for fishes is influenced by the geomorphic structure of watersheds (e.g., Intrinsic Potential models; Bidlack et al. 2014), will likely improve estimates of production patterns.

A new way to map fish production across riverscapes

The approach outlined here represents a new way to map freshwater production of salmon or any other species that are migratory and occupy complex riverscapes. Production of salmon is heterogeneous across space and time, and such heterogeneity acts to buffer the overall productivity of salmon at aggregate levels of population structure and habitat complexity (e.g.,

regional vs. local) from perturbation. This phenomenon has been likened to a portfolio effect, where habitat complexity, locally adapted populations, and differential responses of those populations to change, all contribute to spreading the risk of an ecosystem service (e.g., salmon production) across space and time at aggregated scales (Schindler et al. 2010, 2015). Insights into how this production is distributed across space and time, however, are difficult to obtain, particularly at fine temporal and spatial scales. Similarly, because salmon populations exhibit variation in their age structure (i.e., salmon from the same cohort may spend a different amount of time in the freshwater and ocean before returning to the spawning grounds, denoted by number of years spent in each environment), their production patterns are also apportioned by age. Rarely, however, has the production of salmon been apportioned at finer timescales, such as between different habitat-use strategies during the juvenile freshwater life phase (but see Walsworth et al. 2014 and Brennan et al. 2015*b*). Thus, although smaller spatial and temporal scales play an important role in understanding habitat use by individual juvenile salmon that recruit to adulthood (Bourret et al. 2016), insights have been limited to relatively coarse scales due to the resolution of current methodologies to resolve individual populations in fishery harvests and our ability to monitor across multiple scales simultaneously.

Using a geographically continuous assignment approach we were able to explicitly match individuals to specific habitats during specific time periods. Because this analysis was done on fishery harvests taken at the river's terminus during the annual spawning migration of adults, the sample represents a complex mixture of fish originating from a vast array of potential habitats and potentially exhibiting different life history strategies. Being able to apportion such aggregates provides a powerful way to evaluate the importance of different habitats over time for the overall productivity of populations. For example, the individuals of different age returning in 2011 to the Nushagak River experienced the freshwater conditions of different years (2007, 2006, and 2005). The production heat maps of the different age classes indicate that, although the age 1.3 and 1.4 fish showed similar geographic patterns, the age 1.5 fish did not (production for the 1.5 age class was weighted toward the AAR tributaries along the eastern margin of the river basin; Fig. 4). Because analyses like the ones outlined here explicitly link individuals to habitats in time, they provide a way to evaluate how environmental parameters of such habitats affect production. Perhaps more importantly, if such analyses were extended across multiple years, the brood tables of each year contributing to the annual returns of adults could be reconstructed at spatial and temporal scales not usually accessible via other methods. Effective conservation that takes into account the lessons and insights of how portfolio effects buffer ecological systems is dependent on ways to quantify how productivity is distributed across space and time at multiple scales. The approach outlined here provides a viable framework to do so for migratory fishes which inhabit isotopically or chemically heterogeneous environments.

Acknowledgments

This work was funded by the Bristol Bay Regional Seafood Development Association (BBRSDA) and the Bristol Bay Science Research Institute (BBSRI). Thank you to Hannah Vander Zanden, Gabriel Bowen, Michael Wunder, and Stephen Good and the faculty and staff of the 2015 Spatial Short Course at the University of Utah for their financial support and training of S. R. Brennan in isoscape modeling. Thank you to Thure Cerling, Jeff Hollenbeck, Gordon Holtgrieve, and James Thorson for helpful conversations during the preparation of these analyses and to Tim Walsworth and Tim Cline for their assistance with R code. Thank you to Hannah Vander Zanden and one anonymous reviewer for their reviews of this manuscript.

Literature Cited

Barnett-Johnson, R., T. E. Pearson, F. C. Ramos, C. B. Grimes, and R. B. MacFarlane. 2008. Tracking natal origins of salmon using isotopes, otoliths, and landscape geology. Limnology and Oceanography 53:1633–1642.

Bidlack, A. L., L. E. Benda, T. Miewald, G. H. Reeves, and G. McMahan. 2014. Identifying suitable habitat for chinook salmon across a large, glaciated watershed. Transactions of the American Fisheries Society 143:689–699.

Bourret, S. L., C. C. Caudill, and M. L. Keefer. 2016. Diversity of juvenile Chinook salmon life history pathways. Reviews in Fish Biology and Fisheries 26:375–403.

Bowen, G. J., Z. F. Liu, H. B. Vander Zanden, L. Zhao, and G. Takahashi. 2014. Geographic assignment with stable isotopes in IsoMAP. Methods in Ecology and Evolution 5: 201–206.

Brennan, S. R., D. P. Fernandez, C. E. Zimmerman, T. E. Cerling, R. J. Brown, and M. J. Wooller. 2015*a*. Strontium isotopes in otoliths of a non-migratory fish (slimy sculpin): implications for provenance studies. Geochimica Et Cosmochimica Acta 149:32–45.

Brennan, S. R., C. E. Torgersen, J. P. Hollenbeck, D. P. Fernandez, C. K. Jensen, and D. E. Schindler. 2016. Dendritic network models: Improving isoscapes and quantifying influence of landscape and in-stream processes on strontium isotopes in rivers. Geophysical Research Letters 43:5043–5051.

Brennan, S. R., C. E. Zimmerman, D. P. Fernandez, T. E. Cerling, M. V. McPhee, and M. J. Wooller. 2015*b*. Strontium isotopes delineate fine-scale natal origins and migration histories of Pacific salmon. Science Advances 1:e1400124.

Campana, S. E. 1999. Chemistry and composition of fish otoliths: pathways, mechanisms and applications. Marine Ecology Progress Series 188:263–297.

Cryan, P. M., C. A. Stricker, and M. B. Wunder. 2014. Continental-scale, seasonal movements of a heterothermic migratory tree bat. Ecological Applications 24:602–616.

Dann, T. H., C. Habicht, T. T. Baker, and J. E. Seeb. 2013. Exploiting genetic diversity to balance conservation and harvest of migratory salmon. Canadian Journal of Fisheries and Aquatic Sciences 70:785–793.

Elsdon, T. S., B. K. Wells, S. E. Campana, B. M. Gillanders, C. M. Jones, K. E. Limburg, D. H. Secor, S. R. Thorrold, and B. D. Walther. 2008. Otolith chemistry to describe movements and life-history parameters of fishes: Hypotheses, assumptions, limitations and inferences. Oceanography and Marine Biology: An Annual Review 46:297–330.

Flockhart, D. T. T., L. I. Wassenaar, T. G. Martin, K. A. Hobson, M. B. Wunder, and D. R. Norris. 2013. Tracking multi-generational colonization of the breeding grounds by monarch butterflies in eastern North America. Proceedings. Biological Sciences 280:20131087.

Garreta, V., P. Monestiez, and J. M. V. Hoef. 2010. Spatial modelling and prediction on river networks: Up model, down model or hybrid? Environmetrics 21:439–456.

Griffiths, J. R., et al. 2014. Performance of salmon fishery portfolios across western North America. Journal of Applied Ecology 51:1554–1563.

Hegg, J. C., T. Giarrizzo, and B. P. Kennedy. 2015. Diverse early life-history strategies in migratory amazonian catfish: implications for conservation and management. PLoS ONE 10:e0129697.

Hegg, J. C., B. P. Kennedy, P. M. Chittaro, and R. W. Zabel. 2013. Spatial structuring of an evolving life-history strategy under altered environmental conditions. Oecologia 172: 1017–1029.

Hilborn, R., T. P. Quinn, D. E. Schindler, and D. E. Rogers. 2003. Biocomplexity and fisheries sustainability. Proceedings of the National Academy of Sciences USA 100:6564–6568.

Hobson, K. A. 2011. Isotopic ornithology: a perspective. Journal of Ornithology 152:49–66.

Hobson, K. A., R. Barnett-Johnson, and T. E. Cerling. 2010. Using isoscapes to track animal migration. Pages 273–298 *in* J. B. West, G. J. Bowen, T. E. Dawson, and K. P. Tu, editors. Isoscapes: understanding movement, pattern, and process on earth through isotope mapping. Springer Science, Berlin, Germany.

Hobson, K. A., and D. R. Norris. 2008. Animal migration: a context for using new techniques and approaches. Pages 1–19 *in* K. A. Hobson and L. I. Wassenaar, editors. Tracking animal migration with stable isotopes. Elsevier Inc., Amsterdam, The Netherlands.

Hobson, K. A., D. X. Soto, D. R. Paulson, L. I. Wassenaar, and J. H. Matthews. 2012*a*. A dragonfly (d2H) isoscape for North America: a new tool for determining natal origins of migratory aquatic emergent insects. Methods in Ecology and Evolution 3:766–772.

Hobson, K. A., S. L. Van Wilgenburg, L. I. Wassenaar, and K. Larson. 2012. Linking hydrogen (delta2H) isotopes in feathers and precipitation: sources of variance and consequences for assignment to isoscapes. PLoS ONE 7:e35137.

Hobson, K. A., M. B. Wunder, S. L. Van Wilgenburg, R. G. Clark, and L. I. Wassenaar. 2009. A method for investigating population declines of migratory birds using stable isotopes: origins of harvested lesser scaup in North America. PLoS ONE 4:e7915.

Hobson, K. A., M. B. Wunder, S. L. Van Wilgenburg, R. G. Clark, and L. I. Wassenaar. 2009*b*. A method for investigating population declines of migratory birds using stable isotopes: origins of harvested lesser scaup in North America. PLoS ONE 4:e7915.

Jones, M., T. Sands, S. Morstad, P. Salomone, G. Buck, F. West, T. Baker, and T. Krieg. 2011. 2011 Bristol Bay area annual management report. Fishery Management Report No. 12-21. Alaska Department of Fish and Game, Anchorage, Alaska, USA.

Kennedy, B. P., C. L. Folt, J. D. Blum, and C. P. Chamberlain. 1997. Natural isotope markers in salmon. Nature 387: 766–767.

Koch, P. L., A. N. Halliday, L. M. Walter, R. F. Stearley, T. J. Huston, and G. R. Smith. 1992. Sr isotopic composition of hydroxyapatite from recent and fossil salmon—the record of lifetime migration and diagenesis. Earth and Planetary Science Letters 108:277–287.

Larson, W. A., J. E. Seeb, C. E. Pascal, W. D. Templin, and L. W. Seeb. 2014. Single-nucleotide polymorphisms (SNPs) identified through genotyping-by-sequencing improve genetic stock identification of Chinook salmon (*Oncorhynchus tshawytscha*) from western Alaska. Canadian Journal of Fisheries and Aquatic Sciences 71:698–708.

Levin, S. A. 1992. The problem of pattern and scale in ecology. Ecology 73:1943–1967.

Mercier, L., A. M. Darnaude, O. Bruguier, R. P. Vasconcelos, H. N. Cabral, M. J. Costa, M. Lara, D. L. Jones, and D. Mouillot. 2011. Selecting statistical models and variable combinations for optimal classification using otolith microchemistry. Ecological Applications 21:1352–1364.

Muhlfeld, C. C., S. R. Thorrold, T. E. McMahon, and B. Marotz. 2012. Estimating westslope cutthroat trout (*Oncorhynchus clarkii lewisi*) movements in a river network using strontium isoscapes (vol 69, pg 906, 2012). Canadian Journal of Fisheries and Aquatic Sciences 69:1129–1130.

Peterson, E. E., and J. M. Ver Hoef. 2010. A mixed-model moving-average approach to geostatistical modeling in stream networks. Ecology 91:644–651.

Royle, J. A., and D. R. Rubenstein. 2004. The role of species abundance in determining breeding origins of migratory birds with stable isotopes. Ecological Applications 14:1780–1788.

Runge, C. A., T. G. Martini, H. P. Possingham, S. G. Willis, and R. A. Fuller. 2014. Conserving mobile species. Frontiers in Ecology and the Environment 12:395–402.

Schindler, D. E., J. B. Armstrong, and T. E. Reed. 2015. The portfolio concept in ecology and evolution. Frontiers in Ecology and the Environment 13:257–263.

Schindler, D. E., R. Hilborn, B. Chasco, C. P. Boatright, T. P. Quinn, L. A. Rogers, and M. S. Webster. 2010. Population diversity and the portfolio effect in an exploited species. Nature 465:609–612.

Sturrock, A. M., E. Hunter, J. A. Milton, R. C. Johnson, C. P. Waring, C. N. Trueman, and E. Leder. 2015. Quantifying physiological influences on otolith microchemistry. Methods in Ecology and Evolution 6:806–816.

van Dijk, J. G. B., W. Meissner, and M. Klaassen. 2014. Improving provenance studies in migratory birds when using feather hydrogen stable isotopes. Journal of Avian Biology 45:103–108.

Vander Zanden, H. B., et al. 2015. Determining origin in a migratory marine vertebrate: a novel method to integrate stable isotopes and satellite tracking. Ecological Applications 25:320–335.

Vander Zanden, H. B., M. B. Wunder, K. A. Hobson, S. L. Van Wilgenburg, L. I. Wassenaar, J. M. Welker, and G. J. Bowen. 2014. Contrasting assignment of migratory organisms to geographic origins using long- term versus year-specific precipitation isotope maps. Methods in Ecology and Evolution 5:891–900.

Ver Hoef, J. M., and E. E. Peterson. 2010. A moving average approach for spatial statistical models of stream networks. Journal of the American Statistical Association 105:6–18.

Walsworth, T. E., D. E. Schindler, J. R. Griffiths, and C. E. Zimmerman. 2014. Diverse juvenile life-history behaviours contribute to the spawning stock of ananadromous fish population. Ecology of Freshwater Fish. http://dx.doi.org/10.1111/eff.12135

Walther, B. D., M. J. Kingsford, M. D. O'Callaghan, and M. T. McCulloch. 2010. Interactive effects of ontogeny, food ration and temperature on elemental incorporation in otoliths of a coral reef fish. Environmental Biology of Fishes 89:441–451.

Walther, B. D., S. R. Thorrold, and J. E. Olney. 2008. Geochemical signatures in otoliths record natal origins of

American shad. Transactions of the American Fisheries Society 137:57–69.
Webster, M. S., P. P. Marra, S. M. Haig, S. Bensch, and R. T. Holmes. 2002. Links between worlds: unraveling migratory connectivity. Trends in Ecology & Evolution 17:76–83.
Whited, D. C., J. S. Kimball, J. A. Lucotch, N. K. Maumenee, H. Wu, S. D. Chilcote, and J. A. Stanford. 2012. A riverscape analysis tool developed to assist wild salmon conservation across the north pacific rim. Fisheries 37:305–314.
Whited, D. C., J. S. Kimball, M. S. Lorang, and J. A. Stanford. 2013. Estimation of juvenile salmon habitat in pacific rim rivers using multiscalar remote sensing and geospatial analysis. River Research and Applications 29:135–148.
Wittenberg, S. R., S. E. Lehnen, and K. Smith. 2013. Use of stable isotopes of hydrogen to predict natal origins of juvenile merlins and northern harriers migrating through the Florida keys. Condor 115:451–455.
Woll, C., D. Albert, and D. Whited. 2014. A preliminary classification and mapping of salmon ecological systems in the Nushagak and Kvichak watersheds, Alaska. The Nature Conservancy. http://www.conservationgateway.org/ConservationByGeography/NorthAmerica/UnitedStates/alaska/sw/science/fishhabitat/Pages/default.aspx
Wunder, M. B. 2010. Using isoscapes to model probability surfaces for determining geographic origins. Pages 251–270 *in* J. B. West, G. J. Bowen, T. E. Dawson, and K. P. Tu, editors. Isoscapes: understanding movement, pattern, and process on earth through isotope mapping. Springer, Berlin, Germany.
Wunder, M. B. 2012. Determining geographic patterns of migration and dispersal using stable isotopes in keratins. Journal of Mammalogy 93:360–367.
Wunder, M. B., and D. R. Norris. 2008. Improved estimates of certainty in stable-isotope-based methods for tracking migratory animals. Ecological Applications 18:549–559.

Supporting Information

Additional supporting information may be found in the online version of this article at http://onlinelibrary.wiley.com/doi/10.1002/eap.1474/full